

THESIS FOR THE DEGREE OF DOCTOR OF PHILOSOPHY

CO<sub>2</sub> Capture using Chemical-Looping Combustion  
– Operational Experience with Gaseous and Solid Fuels

CARL LINDERHOLM

Department of Energy and Environment

CHALMERS UNIVERSITY OF TECHNOLOGY

Gothenburg, Sweden 2011

CO<sub>2</sub> Capture using Chemical-Looping Combustion –  
Operational Experience with Gaseous and Solid Fuels

CARL LINDERHOLM  
ISBN 978-91-7385-518-1

© CARL LINDERHOLM, 2011.

Doktorsavhandlingar vid Chalmers tekniska högskola  
Ny serie nr 3199  
ISSN 0346-718X

Department of Energy and Environment  
Chalmers University of Technology  
SE-412 96 Gothenburg  
Sweden  
Telephone + 46 (0)31-772 1000

*Cover: CLC reactor systems used in the experiments:*

*10 kW unit for gaseous fuel (left)*  
*300 W unit for gaseous fuel (center)*  
*10 kW unit for solid fuel (right)*

Chalmers Reproservice  
Gothenburg, Sweden 2011

# CO<sub>2</sub> Capture using Chemical-Looping Combustion – Operational Experience with Gaseous and Solid Fuels

CARL LINDERHOLM

Department of Energy and Environment  
Chalmers University of Technology

## ABSTRACT

CO<sub>2</sub> capture and storage has been proposed as an alternative to mitigate global warming. Chemical-looping combustion (CLC) is an unmixed combustion concept where fuel and combustion air are kept separate by means of an oxygen carrier, and the CO<sub>2</sub> capture is inherently achieved. The work in this thesis focuses on the experimental evaluation of different oxygen carriers and fuels in three CLC reactors. These continuous units are based on interconnected fluidized-bed technology and feature a fuel reactor (FR) and an air reactor (AR) as the principal reaction chambers. Fuel is oxidized to CO<sub>2</sub> and H<sub>2</sub>O in the FR with oxygen supplied by the oxygen carrier, which is based on metal oxide. Oxygen-carrier particles are then re-oxidized in the AR.

A 10 kW chemical-looping combustor for *gaseous fuels* was used to evaluate the long-term performance of different Ni-based oxygen carriers. The most important findings concern particles prepared by spray-drying, which were subjected to more than 1000 h of operation with natural gas as fuel. Fuel conversion was high, and increased with (a) decreased circulation, and (b) increased fuel-reactor temperature. Combustion efficiency close to 99% was accomplished using these spray-dried particles. At the end of the test series, the continuous loss of fine material was 0.003%/h, which corresponds to a particle life time of 33000 h. Experiments in a 300 W chemical-looping combustor for gaseous fuels investigate the possibility to optimize the methane conversion – while retaining the oxygen-transport capacity – by mixing different NiO-based oxygen carriers. The study confirmed that such optimization is indeed feasible.

A 10 kW CLC unit designed for *solid fuels* was used for both continuous and batch tests. In the continuous tests, three oxygen carriers were used; (a) ilmenite, an iron-titanium mineral, (b) ilmenite in combination with limestone, and (c) manganese ore. Generally, longer residence time of the fuel and increased temperature in the FR had a beneficial effect on gasification. Compared to ilmenite, the use of ilmenite+limestone as oxygen carrier improved gas conversion as well as the rate of char gasification. It was shown that this result was due to the effect of limestone on the water-gas shift equilibrium. In another study, in-bed fuel feed was found to significantly improve gas conversion, mainly caused by increased contact between the oxygen carrier and volatile gases produced in the fuel chute. The use of a manganese ore as oxygen carrier greatly enhanced the rate of gasification. Furthermore, gas conversion also improved using the manganese ore. A concern with the manganese ore is the large production of fines. The batch tests in the 10 kW unit involved the feeding of five fuels to the FR in batches of 20-25 g at four temperatures, using ilmenite as oxygen carrier. By using devolatilized fuel, it was possible to determine (a) oxygen demand associated with syngas from char gasification as well as (b) kinetics of gasification. The minimum oxygen demand for char was found to be around 5%.

Keywords: CO<sub>2</sub> capture, chemical-looping combustion (CLC), oxygen carrier, nickel oxide, manganese ore, ilmenite, natural gas, coal, interconnected fluidized beds.

## List of publications

This thesis is based on the work contained in the following papers, referred to by Roman numerals in the text:

- I. Linderholm, C., Abad, A., Mattisson, T., and Lyngfelt, A., 160 h of chemical-looping combustion in a 10 kW reactor system with a NiO-based oxygen carrier, *International Journal of Greenhouse Gas Control*, Volume 2, Issue 4, October 2008, Pages 520-530.
- II. Linderholm, C., Mattisson, T., and Lyngfelt, A., Long-term integrity testing of spray-dried particles in a 10-kW chemical-looping combustor using natural gas as fuel, *Fuel*, Volume 88, Issue 11, November 2009, Pages 2083-2096.
- III. Linderholm, C., Jerndal, E., Mattisson, T., and Lyngfelt, A., Investigation of NiO-based mixed oxides in a 300-W chemical-looping combustor, *Chemical Engineering Research and Design*, Volume 88, Issues 5-6, May-June 2010, Pages 661-672.
- IV. Linderholm, C., Cuadrat, A., and Lyngfelt, A., Chemical-looping combustion of solid fuels in a 10 kW<sub>th</sub> pilot – batch tests with five fuels, *Energy Procedia*, Volume 4, 2011, Pages 385-392.
- V. Cuadrat, A., Linderholm, C., Abad, A., Lyngfelt, A., and Adánez, J., Influence of limestone addition in a 10 kW<sub>th</sub> Chemical-Looping Combustion unit operated with pet coke, *submitted for publication in Energy & Fuels*.
- VI. Linderholm, C., Lyngfelt, A., Cuadrat, A., and Jerndal, E., Chemical-looping combustion of solid fuels – operation in 10 kW unit with two fuels, above-bed and in-bed fuel feed and two oxygen carriers, manganese ore and ilmenite, *Submitted for publication in Fuel*.

## Contribution report

- I. Principal author. Experimental work and data evaluation.
- II. Principal author. Experimental work and data evaluation.
- III. Principal author. Experimental work in 300 W CLC unit and data evaluation.
- IV. Principal author. Experimental work and data evaluation.
- V. Co-author. Experimental work in 10 kW unit.
- VI. Principal author. Experimental work and data evaluation.

## Related publications not included in the thesis

- Linderholm, C., Lyngfelt, A., Béal, C., Trikkel, A., Kuusik, R., Jerndal, E., and Mattisson, T., Chemical-looping combustion with natural gas using spray-dried NiO-based oxygen carriers, in *Carbon Dioxide Capture for Storage in Deep Geological Formations, Volume 3, Advances in CO<sub>2</sub> Capture and Storage Technology (2004-2009)* L. I. Eide (Ed.), October 2009, Pages 67-74.
- Shulman, A., Linderholm, C., Mattisson, T. and Lyngfelt, A., High Reactivity and Mechanical Durability of NiO/NiAl<sub>2</sub>O<sub>4</sub> and NiO/NiAl<sub>2</sub>O<sub>4</sub>/MgAl<sub>2</sub>O<sub>4</sub> Oxygen Carrier Particles Used for Over 1000 Hours in a 10 kW CLC Reactor, *Industrial & Engineering Chemistry Research, Volume 48, 2009, Pages 7400-7405.*
- Berguerand, N, Lyngfelt, A., Markström, P., and Linderholm, C., Chemical-Looping Combustion of Solid Fuels in a 10 kW<sub>th</sub> Unit. *1<sup>st</sup> International Conference on Chemical Looping, Lyon, 17-19 March 2010.*
- Mattisson, T., Jerndal, E., Linderholm, C., and Lyngfelt, A., Reactivity of a spray-dried NiO/NiAl<sub>2</sub>O<sub>4</sub> oxygen carrier for chemical-looping combustion, *submitted for publication.*



## Acknowledgements

My appreciation and gratitude are conveyed to the people listed below, who all contributed to the work presented in this thesis.

**Professor Anders Lyngfelt**, my supervisor, for giving me the opportunity to work with things I care a great deal about, your knowledge and passionate guidance throughout the work. I am truly grateful.

**Assistant Professor Tobias Mattisson**, my co-supervisor, for great support, guidance, and for your enthusiasm.

**My colleagues in the CLC group**, especially Nicolas Berguerand, Magnus Rydén, Pontus Markström, Patrick Moldenhauer and Ulf Stenman, for providing such joyful company in the lab, and Erik Jerndal, for fruitful collaboration over the years (co-author Papers III and VI).

**My dear Spanish colleagues** and co-authors, Ana Cuadrat (Papers IV-VI), and Alberto Abad (Papers I and V) at CSIC, for excellent cooperation.

Ulrik Rosén at TCG for his availability and his ability to fix everything on our chemical-looping combustors.

All unmentioned colleagues at the Division of Energy Technology for offering such a friendly and supportive working atmosphere.

Per Croona at Höganäs, for grinding the manganese ore pro-bono and Dan Hedkvist at SSAB for providing 30 kg metallurgical coke.

My financiers, the ÉCLAIR Project (RFC-PP-07011), financed by the Research Fund for Coal & Steel, and the EU-financed research projects ENCAP (SE56-2004-502666), and CLC Gas Power (contract number 019800).

My brother Pontus, for fresh perspectives on academic writing.

My precious family; the affectionate Ivar, Singing Signe, and my sweet, loving, and funny wife, Elin – you had me at suckiestbunchofsucks.

## Table of Contents

<b>1. Introduction</b> .....	<b>1</b>
1.1 CO <sub>2</sub> emissions and power generation.....	1
1.2 Global warming.....	2
1.3 The greenhouse effect .....	4
1.3.1 Effect of increasing concentration of CO <sub>2</sub> on surface temperature .....	5
1.4 Reducing CO <sub>2</sub> emissions.....	7
1.5. Carbon capture and storage (CCS) .....	8
1.5.1 Cost of CCS .....	8
1.5.2 CO <sub>2</sub> storage.....	9
1.5.3 CO <sub>2</sub> transportation.....	10
1.5.4 CO <sub>2</sub> capture .....	10
1.6 Chemical-looping combustion: overview and background.....	11
1.6.1 CFB technology applied to combustion of solid fuels .....	13
1.6.2 Process studies of CLC with gaseous fuels.....	14
1.6.3 The road to full-scale CLC.....	15
1.7 Relevance and scope of thesis .....	15
<b>2. Theory</b> .....	<b>17</b>
2.1 Solids circulation and $\Delta X$ .....	18
2.2 Oxygen carriers for CLC/CLOU .....	18
2.2.1 CLOU and Mn-based oxygen carriers.....	20
2.2.2 NiO-based oxygen carriers and natural gas as fuel .....	21
2.2.3 Ilmenite with solid fuels .....	22
2.3 Lifetime of oxygen carrier .....	22
<b>3. Experimental</b> .....	<b>24</b>
3.1 Reactor systems.....	24
3.1.1 Construction material for reactor system.....	25
3.1.2 Solids circulation .....	26
3.1.3 Gas leakage.....	27
3.2 Fuels.....	28
3.2.1 Gaseous fuel .....	28
3.2.2 Solid fuel .....	28
3.3 Oxygen carriers .....	28
3.3.1 Oxygen carriers used in experiments with gaseous fuels.....	29
3.3.2 Oxygen carriers used in solid-fuel experiments.....	31

3.4 Gas measurements, definitions and analysis .....	32
3.4.1 Data evaluation with gaseous fuel .....	32
3.4.2 Data evaluation with solid fuel.....	33
<b>4. Results .....</b>	<b>36</b>
4.1 Natural gas experiments.....	36
4.1.1 Papers I and II: long-term tests in Gas-10 kW.....	36
4.1.2 Paper III: comparison of oxygen carriers .....	39
4.2 Solid fuel experiments .....	40
4.2.1 Paper IV: batch tests in SF-10 kW .....	40
4.2.2 Papers V and VI: continuous tests in SF-10 kW .....	40
<b>5. Discussion .....</b>	<b>44</b>
5.1 Experiments with natural gas .....	44
5.2 Experiments with solid fuels.....	44
<b>6. Conclusions.....</b>	<b>46</b>
6.1 Experiments with gaseous fuels .....	46
6.1.1 Long-term tests in Gas-10 kW using N-IFP (Paper I) .....	46
6.1.2 Long-term tests in Gas-10 kW using N-VITO and N-VITOMg (Paper II) .....	46
6.1.3 Comparison of Ni-based oxygen carriers (Paper III) .....	47
6.2 Experiments with solid fuels.....	47
6.2.1 Batch experiments (Paper IV).....	48
6.2.2. Continuous experiments (Papers V and VI).....	48
<b>References .....</b>	<b>50</b>



# 1. Introduction

The availability of useful energy forms such as electricity and heat constitutes a fundamental requirement of industrialized society as we know it, and is strongly correlated with life expectancy and standard of living [1]. On a global scale, more than 80% of the primary energy supply is satisfied by fossil fuels [2], which upon conversion, through combustion, produce CO<sub>2</sub> as waste. The combustion process is essentially the same in a 2000 MW<sub>th</sub> coal power plant as in a candle in your home: a hydrocarbon fuel is mixed with oxygen and transformed into carbon dioxide (and water),



Carbon dioxide, however, is a greenhouse gas, and the problem addressed by this thesis is how to prevent CO<sub>2</sub> from reaching the atmosphere.

## 1.1 CO<sub>2</sub> emissions and power generation

When industrialization took off, so did CO<sub>2</sub> emissions (Fig. 1). CO<sub>2</sub> is released into the atmosphere, where a lot of it remains for a long time. Consequently, the globally averaged CO<sub>2</sub> concentration in the atmosphere (on dry air) has increased from the pre-industrial (AD 1000-1750) levels of 275-285 ppm, to a current 392 ppm [3] – a 40% increase. As we shall see, there are many reasons to believe that the extra CO<sub>2</sub> in the atmosphere will cause the Earth's surface temperature to increase.

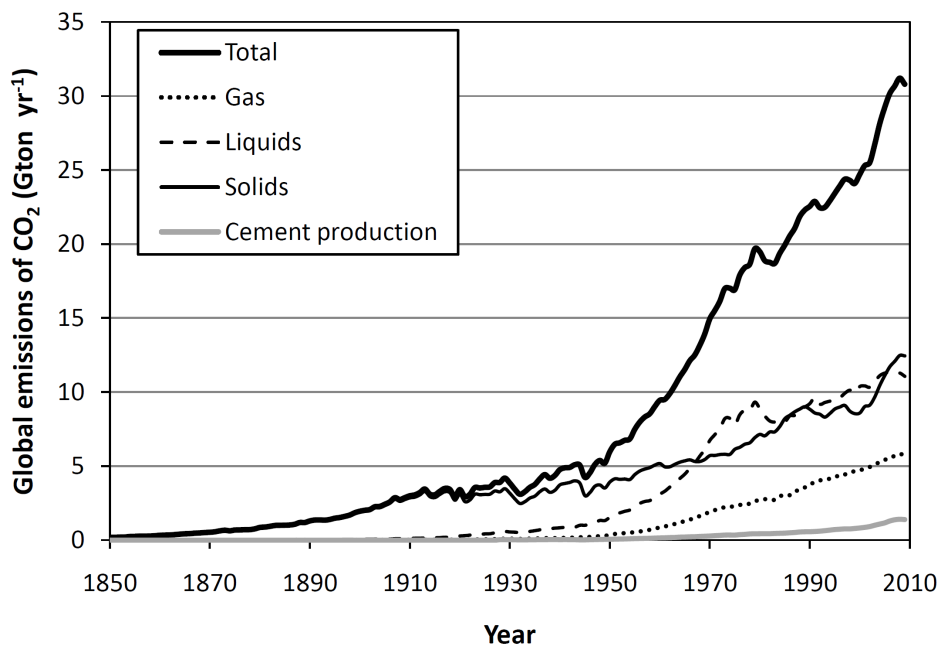
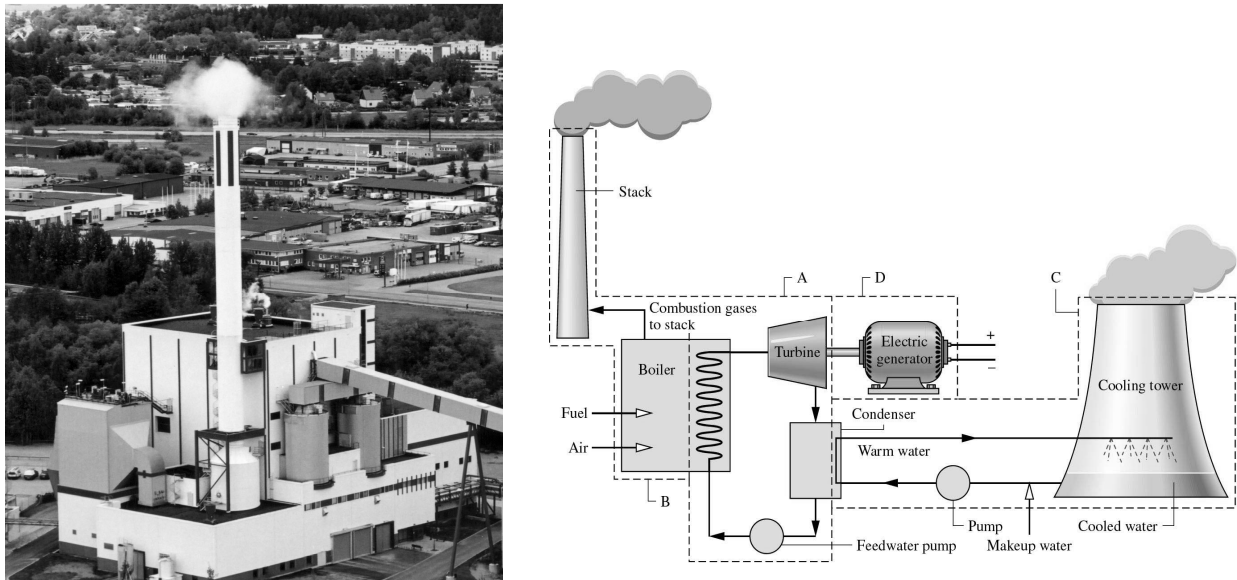


Figure 1. Annual global CO<sub>2</sub> emissions from fossil fuels and cement production, 1850-2009. Values for 2008 and 2009 are preliminary. Source: Boden *et al.* [4].

Almost half of the world's CO<sub>2</sub> emissions come from power plants burning fossil fuels [5]. Such plants generate more than two thirds of the global electricity [2]. Fossil-fuel fired power plants often utilize a steam cycle, whereby heat evolved in the combustion process is transferred to compressed H<sub>2</sub>O. Evaporated, high-pressure steam is then allowed to expand in a turbine, generating work against the turbine blades, which in turn force the turbine axis to rotate, and the energy can be converted to electricity in a generator (Fig. 2, right).



**Figure 2. Power plant using carbonaceous fuel (left), and schematic view of power generation by combustion of carbonaceous fuel (right). CO<sub>2</sub> is released to the atmosphere through the stack. The particular plant on the left is a combined heat and power plant (Eskilstuna kraftvärmeverk).**

The topic of this thesis is chemical-looping combustion (CLC), which is a combustion process where the generated CO<sub>2</sub> is inherently captured. The motive for CO<sub>2</sub> capture, which is the first step in *carbon capture and storage* (CCS) – a global warming mitigation strategy – will be discussed further below. Future power generation applications could be based on the CLC technique.

## **1.2 Global warming**

There is strong evidence that the global average surface temperature is increasing and that the sea level is rising (Fig 3). Of the twelve years 1995-2006, eleven rank among the twelve warmest years since 1850, *i.e.* since the beginning of instrumentally recorded temperature [6]. The fourth Assessment Report from IPCC states that, “since 1750, it is extremely likely that humans have exerted a substantial warming influence on climate” [6]. In this case, “extremely likely” translates to a probability of more than 95%.

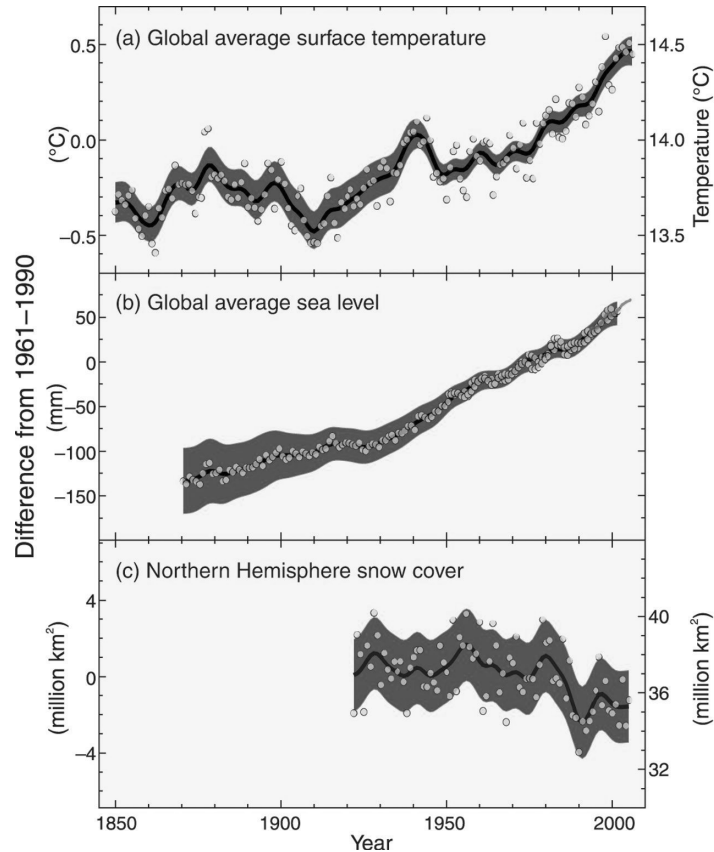


**Figure 3. Observed changes in (a) global average surface temperature; (b) global average sea level from tide gauge and satellite data; and (c) Northern Hemisphere snow cover for March-April. All differences are relative to corresponding averages for the period 1961-1990. Smoothed curves represent decadal averaged values while circles show yearly values. The shaded areas are the uncertainty intervals estimated from a comprehensive analysis of known uncertainties (a and b) and from the time series (c). From AR4 (Synthesis report), IPCC [6].**

Without the ability to perform controlled experiments on our climate and atmosphere, it is difficult to prove that anthropogenic emissions of CO<sub>2</sub> and other greenhouse gases are the primary source of climate change. (Except for mathematics, science is not an absolute language – it is merely a set of more or less elaborate explanations, which have to be continuously compared to nature, where each successful prediction adds to the evidence supporting the scientific explanation.)

At present, there is very strong support within the scientific community for human-induced global warming [7]. The reports of the IPCC, which are frequently cited throughout this chapter, have come to represent the “standard” view of climate change. In order to give room for the essential doubt, a couple of contrarian arguments will be raised here: (a) it is *possible* that the observed warming can be attributed to “natural variability”, and (b) there is

substantial uncertainty in the climate models, especially related to clouds, and that, as a result, it is difficult to predict the future climate.

Sea level rise, polar melt down, droughts, floods, increased intensity of tropical cyclones and reduced diversity of ecosystems, are all probable outcomes of continued global warming [8]. Given that the consequences of continued global warming are so dreadful, developing mitigation strategies has been given high priority by politicians around the world. CLC, as a CO<sub>2</sub> capture technology, is part of such efforts.

### ***1.3 The greenhouse effect***

The greenhouse effect is caused by naturally occurring atmospheric gases, such as H<sub>2</sub>O and CO<sub>2</sub>, called greenhouse gases (GHGs). Without greenhouse gases, the average temperature on the Earth's surface would be approximately 255 K, *i.e.* approximately 33 K colder than at present and well below the freezing point of water, which means that life might not have evolved. Hence, the existence of CO<sub>2</sub> in the atmosphere is vital to living organisms on Earth.

So, how does the greenhouse effect work? All objects at a temperature above absolute zero emit thermal radiation. The temperature of an object determines the frequency distribution of the radiation. In general, the hotter the object is, the higher the frequency and hence the shorter the wavelength. The climate on Earth is powered by the Sun's high-frequency thermal radiation, ranging from visible to ultraviolet. The surface temperature of the Earth is significantly lower than that of the Sun, therefore the Earth radiates in the infrared (IR) part of the spectrum (mainly 4-50 μm). A major portion of the radiation emitted from the surface is absorbed by the atmosphere and then re-radiated back to Earth. Of course, when the climate is at equilibrium, this does not upset the overall radiation balance; incoming radiation must equal outgoing radiation, but the effect of the atmosphere is to increase the surface temperature, since the temperature must be sufficiently high to generate thermal radiation equivalent to the sum of incoming solar and infrared radiation. This phenomenon is commonly referred to as the greenhouse effect.

The most important greenhouse gases are, by order of impact, water vapor, carbon dioxide, ozone, methane and nitrous oxide, all of which are naturally occurring. The amount of water vapor in the atmosphere depends mainly on air temperature. The reason why the two most abundant atmospheric species, N<sub>2</sub> and O<sub>2</sub> – comprising 99% of the dry atmosphere – exert almost no greenhouse effect, ultimately comes down to quantum mechanics: atoms and molecules can only accept or deliver photons in discrete energy levels, and many diatomic molecules, *e.g.* N<sub>2</sub> and O<sub>2</sub>, having a limited number of vibrational and rotational energies, are transparent to IR radiation from Earth. Instead, it is the rarer and more complex – primarily

tri-atomic – atmospheric molecules that absorb IR-radiation from Earth and hence ensure an average surface temperature above the freezing point of water.

### **1.3.1 Effect of increasing concentration of CO<sub>2</sub> on surface temperature**

Anthropogenic emissions of GHGs compromise the radiative balance of the Earth-atmosphere system, and the magnitude of the compromise is usually described in terms of radiative forcing. The radiative forcing relates the *change* in the radiative balance at the tropopause, *i.e.* at the top of the troposphere, for example between 1750 and 2011; a change that is brought about by an alteration in, for example, the concentration of a GHG, the occurrence of aerosols (particles), incident solar radiation, or cloud cover, which affects the fraction of reflected solar light (the albedo). Positive forcings lead to warming of climate and negative forcings lead to cooling. It should be noted that radiative forcings do not necessarily have anthropogenic origin.

The strength of the radiative forcing exercised by the GHGs depends on three main factors [8]:

- (i) The ability of a given gas to absorb infrared radiation,
- (ii) The magnitude of the radiation emitted from the Earth's surface at the wavelengths where the given gas is able to absorb,
- (iii) To what extent other GHGs are already absorbing at the wavelengths where the given gas is able to absorb; some absorption bands may be almost saturated, which means that more or less all IR-radiation emanating from Earth at that frequency is already absorbed or scattered, and hence that an emission of a GHG that absorbs strongly at this frequency will have a relatively small impact on the radiative balance. In contrast, GHGs that absorb in the “atmospheric window” (8-12  $\mu\text{m}$ ), which is far from saturated, will have a more linear relationship between forcing and increase in concentration.

It is clear that CO<sub>2</sub> is the largest single contributor to the change in the radiative balance (Fig. 4). It is also evident that the cloud albedo effect constitutes the largest single uncertainty.

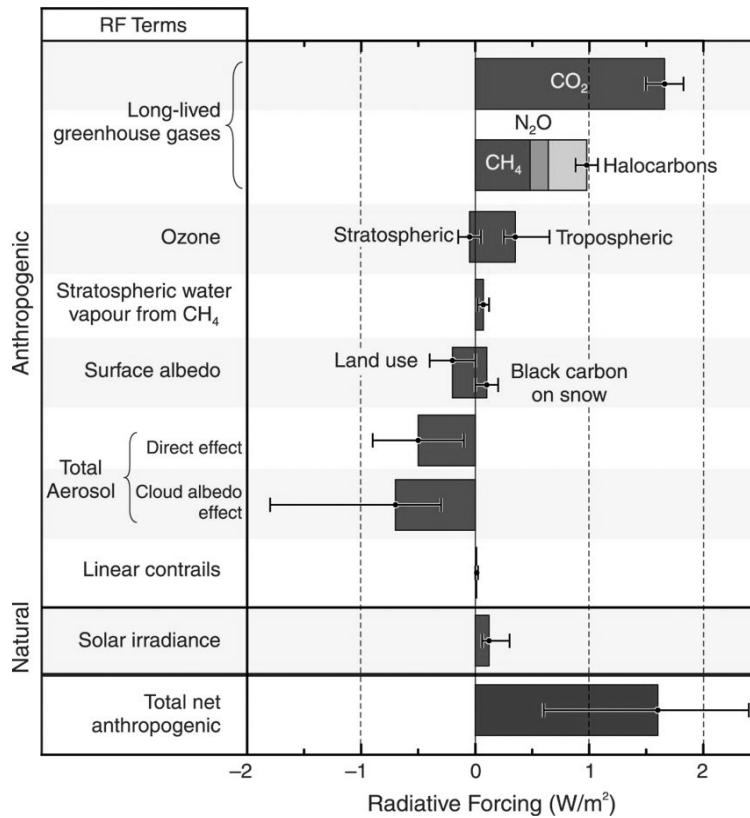


**Figure 4. Summary of the principal components of the radiative forcing of climate change. The values represent the forcings in 2005 relative to the start of the industrial era (about 1750). Human activities cause significant changes in long-lived gases, ozone, water vapor, surface albedo, aerosols and contrails. The only increase in natural forcing of any significance between 1750 and 2005 occurred in solar irradiance. The thin black line attached to each bar represents the range of uncertainty for the respective value. From AR4, IPCC [6].**

It is difficult to translate a radiative forcing into an actual temperature change at Earth's surface. One way to describe this climate response is by introducing the climate sensitivity,  $\lambda$ . Here, the surface temperature change is linearly related to the radiative forcing,

$$\Delta T_s = \lambda \Delta R, \quad (2)$$

which treats the initial and the final climate states as being at equilibrium.  $\Delta T_s$  is the change in global and annual mean surface air temperature, and  $\Delta R$  is the radiative forcing. The reason why climate is difficult to predict is partially explained by the influence of various feedback processes. The feedback is the response of the climate system to the initial change, *i.e.* the response to the radiative forcing. The feedback might amplify or dampen the initial change. The amount of water vapor is projected to be the single largest feedback, and since H<sub>2</sub>O is a GHG, it is a positive feedback. The water-vapor feedback works like this: a positive radiative

forcing will lead to higher temperatures and thus more evaporation, *i.e.* more water vapor in the troposphere, which in turn increases the radiative forcing and consequently the surface temperature will increase as well.

Climate sensitivity is often used in the context of the surface temperature response to a doubling in atmospheric CO<sub>2</sub> concentration, *i.e.* from 275 ppm to 550 ppm. Such a doubling entails a forcing of 3.7 W/m<sup>2</sup>, and without any feedbacks, this would result in a temperature increase of around 1 K [6]. However, due to different kinds of feedbacks, the expected increase, according to the IPCC, is 2-4.5 K [6]. A small number of researchers find lower values for the expected temperature increase. For example, Lindzen *et al.* [9] – while agreeing with the non-feedback case, an increase of 1 K – find the overall feedback processes to give a negative contribution to the warming, and therefore project a < 1 K surface temperature increase for a doubling in CO<sub>2</sub> concentration. The result probably reflects a different treatment of the cloud albedo effect.

#### **1.4 Reducing CO<sub>2</sub> emissions**

In order to mitigate global warming, it is widely accepted that actions must be taken to decrease CO<sub>2</sub> emissions. Many research groups, companies and organizations are working hard to find ways to reduce CO<sub>2</sub> emissions without reducing the world's power consumption. Much effort is being put into different strategies such as:

- Energy efficiency improvements,
- Increasing the use of renewable sources of energy, such as hydro-, wind and solar power,
- Promoting CO<sub>2</sub> uptake in biomass, *e.g.* reforestation,
- Switching from fossil fuels to biomass,
- Expanding the use of nuclear power,
- Large-scale geo-engineering, for example iron fertilization of the oceans in order to promote growth of microorganisms [10]. This option is more controversial since deviations from expected behavior could have devastating effects on ecosystems.

In spite of all these efforts, there are many reasons to believe that fossil fuels will continue to dominate the supply of primary energy for several decades to come [5]. Hence, yet another way to reduce CO<sub>2</sub> emissions has been suggested: combining the use of fossil fuels with CO<sub>2</sub> capture and storage (CCS). In an idealized case, this would yield a “carbon neutral” source of heat and power. By applying CCS to combustion of biofuels, the atmospheric levels of CO<sub>2</sub>

could even be made to decrease (“negative emissions”), since the carbon effectively would be removed from the atmosphere.

### 1.5. Carbon capture and storage (CCS)

Implementation of CCS is feasible on any large stationary source of CO<sub>2</sub>, e.g. power plants. This is good news, since power plants account for 45% of all CO<sub>2</sub> emissions [5]. Other large point sources of CO<sub>2</sub> that could be equipped with CO<sub>2</sub> capture include iron and steel industry, cement production, refineries and petrochemical industry, which together account for another 12% CO<sub>2</sub> emissions. This means that more than 40% of the CO<sub>2</sub> emissions come from small or medium sized sources, from which carbon capture and storage discussed here is not feasible. One option to reduce these smaller-sized emissions would be to convert natural gas to H<sub>2</sub> in large steam-reforming plants, which, if coupled to CCS, would be carbon neutral.

CCS is a novel concept that can be based on proven technology, as discussed below. Fig. 5 shows a general overview of possible CCS systems.

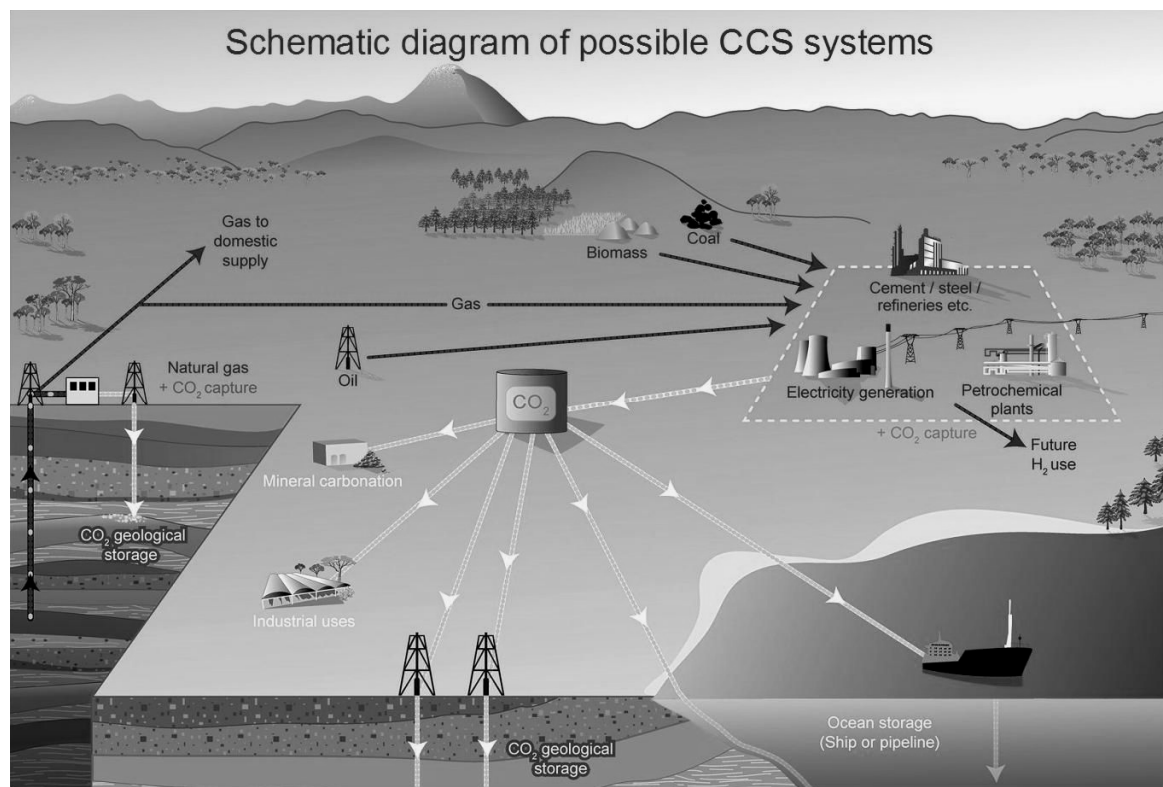


Figure 5. Possible CCS systems, from fossil fuel recovery to storage. From [5].

#### 1.5.1 Cost of CCS

The cost of applying CCS to electricity production is subject to substantial uncertainty [5]. For a plant using pulverized coal (PC), power generation without capture costs 0.04-0.05 US\$/kWh (2002 cost range), whereas a PC plant with capture and geological storage would produce

electricity to a cost of 0.06-0.010 US\$/kWh. *i.e.* essentially a doubling. The major part of the cost increase can be attributed to the capture part of CCS. CO<sub>2</sub> capture from a coal- or gas-fired plant would cost 15-75 US\$/tCO<sub>2</sub> net captured. The combined cost of transportation, storage and monitoring would be 1.6-16.3 US\$/tCO<sub>2</sub> net [5].

### 1.5.2 CO<sub>2</sub> storage

Available options for the final handling of produced CO<sub>2</sub> include underground geological storage, ocean storage and mineral carbonation. Geological storage, which presently seems to be the most plausible alternative, basically means returning the carbon to whence it came. Potential geological storage sites include depleted oil and gas reservoirs, deep unmineable coal seams, deep saline water-saturated reservoir rocks (aquifers), and sites where enhanced oil recovery using CO<sub>2</sub> is practiced. The engineered injection of CO<sub>2</sub> into subsurface geological formations has been undertaken since the 1970s for the purpose of enhanced oil recovery. Storing CO<sub>2</sub> in deep geological formations would thus use technologies that the oil and gas industry has practiced for decades.

It has been suggested, from observations and models, that the leakage rate is likely to be less than 1% of injected CO<sub>2</sub> per 1000 years [5]. If injected into a suitable geological formation at depths below 800 m, a variety of mechanisms would prevent leakage. An essential feature is the presence of caprock, which is a rock of very low permeability that could act as an upper seal and prevent leakage.

The first large-scale CO<sub>2</sub> storage project was started in 1996 by Statoil and its partners at the Sleipner gas field in the North Sea, where almost 1 Mt CO<sub>2</sub> has been injected annually in the Utsira aquifer [5].

Mineral carbonation offers a different kind of storage, involving transformation of gaseous carbon to solid ditto. Examples of reactions include



The products are very stable and the reactions occur naturally, although on geological time-scales. Mineral carbonation is a theoretically appealing option, but it has not been possible to enhance the reaction rate sufficiently to make mineral carbonation a realistic option for large-scale CO<sub>2</sub> reduction.

### 1.5.3 CO<sub>2</sub> transportation

Transportation of CO<sub>2</sub> from production site to storage site should constitute no major obstacle. Large-scale transportation of CO<sub>2</sub> has already been practiced for decades for use in enhanced oil recovery. In USA, 2500 km of pipeline transports an annual amount of more than 40 Mt CO<sub>2</sub> [5]. Both on-shore and off-shore pipelines are feasible. For very long distances, ships offer the most cost-effective option.

### 1.5.4 CO<sub>2</sub> capture

In normal combustion processes, the dry CO<sub>2</sub> concentration is 10-15%. Because more or less undiluted CO<sub>2</sub> is needed for storage, the first step of CCS is the separation of CO<sub>2</sub> from any other gases present in the flue gas, *i.e.* primarily nitrogen.

The capture can be achieved in a number of ways [5], most of which are associated with a substantial energy penalty. As is illustrated in Fig. 6, three major paths to achieve CO<sub>2</sub> separation in a combustion process can be distinguished,

- Post-combustion, where CO<sub>2</sub> is separated from a CO<sub>2</sub>-rich gas stream, *e.g.* the flue gas from a conventional power plant, by for example chemical absorption,
- Pre-combustion, which involves the conversion of a carbon containing fuel to a mixture of CO<sub>2</sub> and H<sub>2</sub>, from which CO<sub>2</sub> is separated prior to combustion, and finally
- Oxyfuel, where the fuel is burnt in a mixture of oxygen and recycled CO<sub>2</sub> instead of air, which requires a primary air separation step, normally achieved in cryogenic air separation unit (ASU).

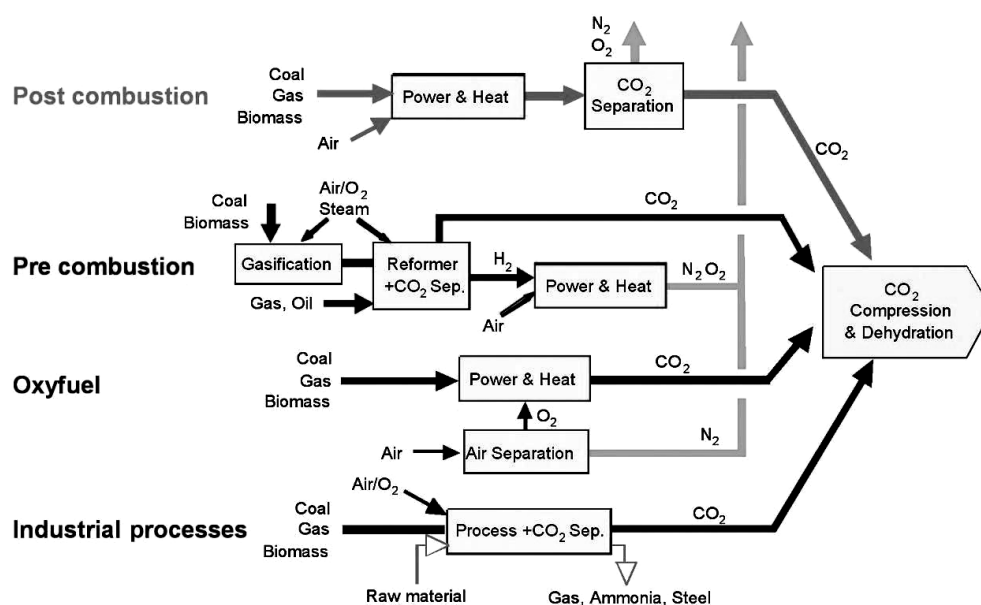


Figure 6. Overview of CO<sub>2</sub> capture processes. From IPCC special report on CCS [5].

The fourth path in Fig. 6 represents CO<sub>2</sub> capture from industrial processes such as the manufacture of steel.

Chemical-looping combustion (CLC), which is the topic of this thesis, is a CO<sub>2</sub> capture technology that is often classified as an oxyfuel process, but could more appropriately be placed in a separate category: unmixed combustion, together with fuel cells. The resemblance of CLC to oxy-fuel processes is small, and no ASU is required. All CLC processes used and discussed in this work utilize two connected fluidized beds, with the oxygen carrier acting as bed material.

### ***1.6 Chemical-looping combustion: overview and background***

The major advantage with chemical-looping combustion is the elimination of the energy-intensive gas separation steps that are associated with other CO<sub>2</sub> capture technologies. The process uses metal-oxide particles, to transfer the oxygen from air to fuel (Fig. 7). In normal combustion processes, flue gases are mixed and the concentration of CO<sub>2</sub> on dry basis is 10-15%, whereas in CLC, CO<sub>2</sub> is obtained in a separate gas stream (Fig. 7). Hence, CLC is a process for fuel conversion with inherent CO<sub>2</sub> separation.

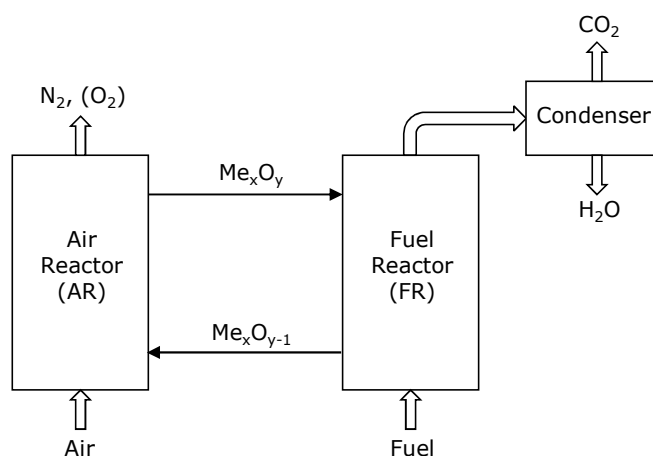


**Figure 7. Schematic representation of chemical-looping combustion. After condensation of the H<sub>2</sub>O produced in the fuel reactor, pure CO<sub>2</sub> is obtained. The gas stream exiting the air reactor contains nitrogen and unreacted oxygen.**

The concept of chemical-looping combustion was first presented in 1954 by Lewis and Gilliland as a means of CO<sub>2</sub> production [11], whereas the use of CLC as a CO<sub>2</sub> capture technology was recognized in 1994 by Ishida *et al.* [12]. In 2001, Lyngfelt *et al.* [13] proposed a CLC reactor design based on circulating fluidized bed (CFB) technology, using metal-oxide particles – an “oxygen carrier” – as bed material. This oxygen carrier would carry oxygen from combustion air to fuel by circulating between the air reactor – a high velocity fluidized bed that

provides the driving force for particle entrainment – and the fuel reactor, which is a bubbling fluidized bed (Fig. 8).

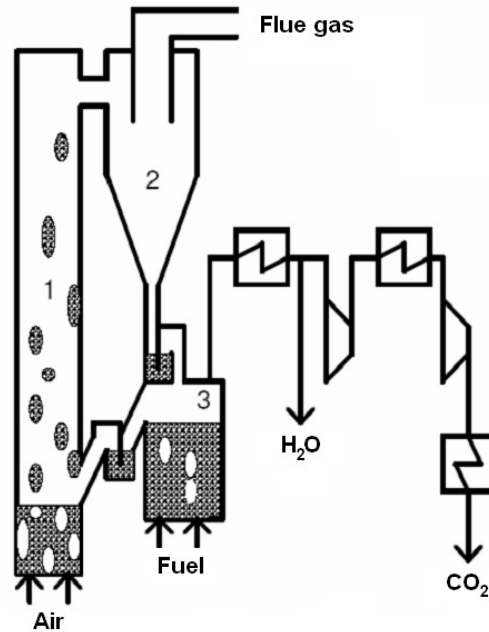


**Figure 8. The CLC process as suggested by Lyngfelt et al [13]. The process is based on CFB-technology with a high velocity riser (1), a cyclone for gas/solids separation (2), and a bubbling bed – the fuel reactor – where the fuel is oxidized with oxygen from the oxygen-carrier particles (3). The fuel-reactor exit gas is successively cooled and compressed in order to condense the water and obtain storage-ready CO<sub>2</sub>.**

CLC with gaseous fuels, *e.g.* natural gas, has been widely investigated, *e.g.* [14,15,16,17]. Since fossil carbon is usually occurring as solids rather than gases or liquids, it is desirable to adapt the CLC process to solid fuels. In chemical-looping with solid fuels, the fuel can be (a) directly introduced into the fuel reactor, or (b) gasified in a primary, separate step, in which case the second step becomes CLC with gaseous fuels. The chemical-looping combustor for solid fuels used in this work is designed for direct fuel introduction. CLC of solid fuels has been demonstrated by Berguerand and Lyngfelt [18,19,20,21], Shen *et al.* [22,23,24], Wu *et al.* [25], and Cuadrat *et al.* [26].

The research on chemical-looping combustion has been summarized in a number of reviews [15,27,28,29], where it is shown that approximately 900 oxygen-carrier materials have been investigated. The actual operational experience in chemical-looping combustors [28] involve totally 12 units of size 0.3-120 kW<sub>th</sub> comprising more than 4000 h of operational experience and 29 different materials.

The CLC concept presented in this thesis is based on circulating fluidized bed (CFB) technology, with the oxygen carrier acting as bed material. A short introduction to fluidization and CFB technology applied to combustion could therefore be useful to the reader.

### 1.6.1 CFB technology applied to combustion of solid fuels

Fluidization is a process in which a bed of particles is converted from a static solid-like state to a dynamic fluid-like state. This transition is brought about by subjecting the particles to an upward fluid flow with a velocity greater than the minimum fluidization velocity ( $u_{mf}$ ) at which point the bed becomes fluid-like.  $u_{mf}$  is reached when the drag force by upward moving gas equals the weight of particles in the bed. The required gas velocity depends on the properties of the gas and particles. Fluidization is used in, for example, (a) fluid catalytic cracking (FCC), where large hydrocarbon molecules are broken down to smaller ones, *e.g.* gasoline, (b) food processing applications, such as drying and freezing, and (c) combustion.

The terminal velocity ( $u_t$ ) is the gas velocity at which the drag force acting on a single particle is equal to the weight of the particle. When  $u_{superficial} > u_t$ , entrainment occurs, which means that particles are carried away from the fluidization vessel by the gas stream. If particles are allowed to return to the bottom of the bed by addition of an external gas/solids separator, a circulating fluidized bed (CFB) is created (Fig. 9).

A growing share of the power generation from fossil fuels takes place in CFB furnaces. CFB is sometimes considered as a “niche” technology, but is slowly emerging as a competitive alternative to more conventional alternatives for power generation by combustion, *e.g.* pulverized coal (PC) boilers. In comparison to PC plants, the low combustion temperature ( $\sim 850^\circ\text{C}$ ) of the CFB minimizes  $\text{NO}_x$  and permits optimum sulfur capture by the simple addition of limestone [30]. Hence, extra equipment (“add-ons”) that conventional coal plants need to capture  $\text{SO}_2$  and  $\text{NO}_x$  is reduced or entirely eliminated in CFB combustion. The circulating solids, *i.e.* sand/limestone, act as a thermal flywheel by storing a large amount of thermal energy, thus providing more isothermal conditions. Yet another advantage of the CFB boiler is the fuel residence time. In PC units, the residence time of the fuel may be as short as 2-3 s [31], whereas in a CFB, the residence time can be very long thanks to the cyclone, which returns heavier, unburned material to the bottom of the furnace. These features explain why the CFB combustor can handle difficult fuels such as discarded tires, pet coke and sewage sludge. Fig. 9 shows a general representation of a circulating fluidized bed, with flow patterns indicated by arrows.

The currently largest commercial CFB boiler, put into operation in 2009, is the 460 MW<sub>e</sub> Łagisza plant in Poland [32], built by Foster Wheeler with a net efficiency of 43% (Fig. 9,

right). It is 48 m high with a horizontal cross section of 28 x 11 m. Boiler designs in size range of 600 – 800 MW<sub>e</sub> are being developed.

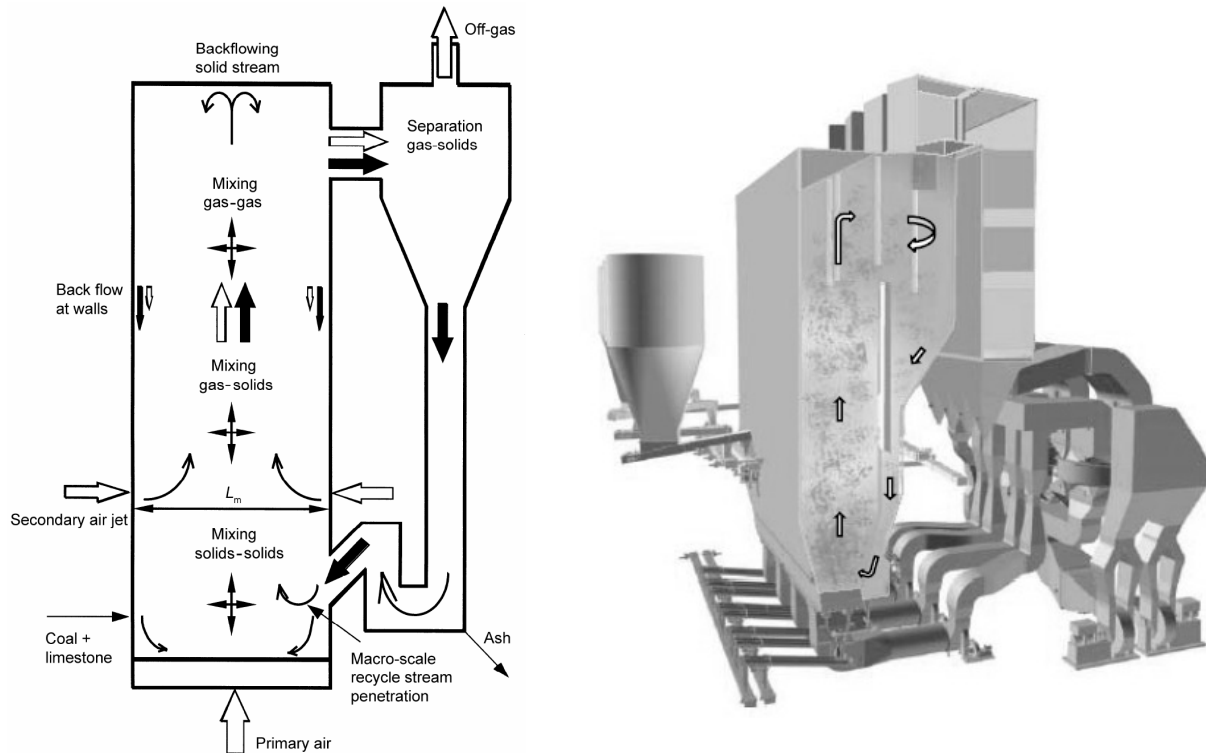


**Figure 9. Left: A schematic CFB-combustor indicating macro-scale mixing and separation processes, (solid arrows: solids; hollow arrows: gas). The furnace is the large chamber to the left [33]. Right: the 460 MW<sub>e</sub> boiler in Łagisza, Poland. Arrows indicate global solids circulation.**

### 1.6.2 Process studies of CLC with gaseous fuels

A number of literature studies have investigated the possibility to combine power cycles with the chemical-looping system. These process simulations have been performed using different types of oxygen carriers and natural gas or synthesis gas as fuel. Reviews of the literature in this area can be found in the doctoral theses of Wolf [34] and Naqvi [35]. The process studies demonstrate that it is theoretically possible to achieve high thermal efficiencies using CLC integrated with CO<sub>2</sub> capture. However, if very high efficiencies are to be reached using gaseous fuels, combined cycle processes involving pressurized fluidized beds would have to be used. It should be pointed out that the temperatures normally used in combined cycles are higher than those at which oxygen carriers usually have been tested.

### **1.6.3 The road to full-scale CLC**

A lot of experimental research on oxygen carriers for CLC has been performed in laboratory batch reactors. Batch tests in laboratory provide vital information on general particle characteristics including reactivity. However, investigations in continuous chemical-looping systems are necessary in order to obtain a more comprehensive understanding of the behaviour of the particles.

CLC is a “young” technology. The 10 kW unit for gaseous fuels used in Papers I-II was the first to show successful continuous operation of chemical-looping combustion. Oxygen carriers had previously only been tested batch-wise in lab, where CLC conditions can be simulated by subjecting particles to alternating oxidizing and reducing conditions. Demonstration of the technology in a continuous unit was a necessity to “prove the concept”, which was the intention of the prototype. This was achieved in 2003. Consequently, until 2003, CLC was merely a paper concept. The chemical-looping combustor for solid fuels used in this work was also the first of its kind and was put into operation in 2006. Recently, a 120 kW CLC pilot for gaseous fuels was built at the Technical University of Vienna, Austria [36].

It should be pointed out that results obtained in the experimental facilities used here may not be representative to what would be obtained in a full-scale system. A large unit could have a 50 m high riser, thus a freeboard containing large amounts of solids which would be expected to give improved contact. Moreover, such a unit would also operate at higher gas velocities, which might improve the mixing. On the other hand, the much larger cross-section area could have negative effect on the contact.

The construction of a full-scale CLC plant using solid fuels based on CFB technology requires successive steps of up-scaling. Currently, two CLC pilots for solid fuels are being constructed at Chalmers (100 kW) and in Darmstadt, Germany (1 MW). If these units show successful operation, further up-scaling to demonstration size (10-100 MW) is not far ahead, which means that the road to full-scale may not be that long for CLC.

### ***1.7 Relevance and scope of thesis***

CLC is a prime contender for CO<sub>2</sub> capture because it can achieve CO<sub>2</sub> separation inherently. Alternative capture technologies require cost-intensive separation steps, either down-stream or up-stream of the combustion.

The work presented in this thesis involves experimental evaluation of oxygen carriers in continuous reactor systems. The large-scale application of CLC is still dependent upon the availability and performance of oxygen carriers. Constructing and operating a power plant with

carbon capture inevitably entails a cost increase, compared to a plant without carbon capture. Because CLC is not as mature as other options for CO<sub>2</sub> capture, the additional costs related to a full-scale CLC plant are therefore, at this point, subject to more uncertainty. The cost increase can be attributed to (a) increased capital cost, *i.e.* mainly the cost for construction of the plant, (b) operating and maintenance cost, which is most likely higher for a novel combustion process such as CLC, and (c) the oxygen carrier. The latter concerns cost of raw material, cost of manufacture (when such is necessary) and lifetime of the carrier. Information about the lifetime of a carrier can be obtained by subjecting a batch of particles to long-term operation and observe the rate of particle degradation. It is then possible to calculate the fractional loss of particles and the lifetime, which can be assumed to be similar in a full-scale system. Consequently, information on lifetime of the carrier is essential for any cost-increase estimate.

The purpose of the work presented in Papers I-III was to investigate the feasibility of making a good oxygen carrier at a reasonable production cost by using commercially available raw materials and commercial preparation methods. The work focuses primarily on the long-term performance of oxygen carriers in continuous CLC operation. The effects on particles of long-term exposure to a CLC environment cannot be otherwise evaluated.

An important difference with solid fuels is the formation of ashes, which means that a large mass flow of ash has to be continuously discharged from the combustion of most solid fuels. This ash discharge, and possibly also fouling by ash, is expected to limit the lifetime of the oxygen carrier. Consequently, oxygen carriers of low cost are studied for solid fuels, and there is also less emphasis on proving a long lifetime of the oxygen carriers.

The purpose of work with solid fuels, Papers IV-VI, was to improve the performance of the existing chemical-looping combustor, increase the level of understanding of CLC with solid fuels by using a variety of different fuels and finally, to investigate to what extent overall performance of the CLC unit could be improved by using a previously untested oxygen carrier with higher reactivity.

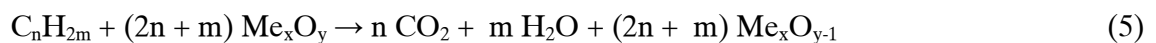
## 2. Theory

The chemical-looping technologies include chemical-looping combustion (CLC), chemical-looping reforming (CLR) and chemical-looping with oxygen uncoupling (CLOU), all of which have the purpose of thermal conversion of fuel with inherent CO<sub>2</sub> capture by means of an oxygen carrier. The solid oxygen carrier, which consists of metal oxide, transfers oxygen from air to fuel. The oxygen carrier circulates in a reactor system composed of a fuel reactor (FR), where oxygen is supplied to fuel by the oxygen carrier, and an air reactor (AR), where the oxygen-carrier particles are regenerated to the oxidized state.

In CLC, the desired output is heat and the desired end-products are therefore CO<sub>2</sub> and H<sub>2</sub>O, whereas in CLR, the purpose is to produce synthesis gas, a mixture of CO and H<sub>2</sub>. In CLR, the air-to-fuel ratio is kept at a low level to prevent the fuel from becoming too oxidized. CLR was first proposed in a patent application 1947 [37] and again by Mattisson and Lyngfelt in 2001 [38] and has since been widely investigated [39,40,41,42,43].

CLOU, chemical-looping with oxygen uncoupling, is closely related to CLC (and CLR) with one crucial difference: gaseous oxygen is released by the oxygen carrier in the FR. For gaseous fuels this means that the fuel oxidation in the FR can potentially occur exclusively in gas phase, and that direct contact of fuel gases with the solids becomes less important. For solid fuels it means that the slow gasification of char can be avoided as the oxygen released can react directly with the char.

In CLC with gaseous fuels, the fuel, *i.e.* natural gas, reacts directly with the metal oxide according to



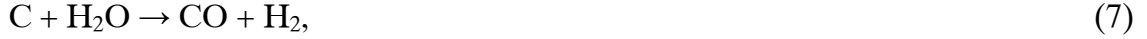
This reaction takes place in the FR and produces only CO<sub>2</sub> and H<sub>2</sub>O. Thus, after condensing the steam, pure CO<sub>2</sub> is obtained. The reduced metal oxide in the oxygen-carrier particles is regenerated in the air reactor,



The flue gas from the air reactor will contain nitrogen and some unreacted oxygen. Reaction (6) is invariably highly exothermic, whereas reaction (5) can be either endo- or exothermic, depending on fuel and on the metal oxide used as oxygen carrier. However, the total amount of heat evolved in reactions (5) and (6) is the same as in conventional combustion.

Adapting the CLC process for solid fuels entails some complications. The solid-solid reaction between the fuel and metal oxide can be neglected. Instead, the process is split up into two

major steps; first the fuel needs to be gasified, reactions (7) and (8), whereupon the gaseous products can react with the oxygen carrier to form carbon dioxide and water, reaction (9).



Atmospheric steam/carbon dioxide gasification of char may take several minutes at 970°C [44], whereas reactions between syngas and most oxygen carriers investigated for CLC are fairly quick [45,46], so it is reasonable to assume that gasification is the rate limiting step in CLC using solid fuels.

### **2.1 Solids circulation and $\Delta X$**

The solids circulation determines the difference in conversion of particles leaving and returning to the air reactor, *i.e.* how much of the available oxygen in the particles that is consumed in the fuel reactor. The degree of oxidation of the particles, also called particle conversion,  $X$ , is defined as the ratio of the amount of available oxygen present in the carrier and the amount of available oxygen present in the carrier when fully oxidized,

$$X = \frac{m_{actual} - m_{red}}{m_{ox} - m_{red}} \quad (10)$$

where  $m_{actual}$  is the actual mass of the carrier in its partially oxidized state,  $m_{ox}$  is the mass of the sample when fully oxidized, and  $m_{red}$  the mass of the sample in the fully reduced form. The particle conversion in the air reactor,  $X_{AR}$ , is larger than that in the fuel reactor,  $X_{FR}$ , during normal combustion conditions. The difference in particle conversion,

$$\Delta X = X_{AR} - X_{FR}, \quad (11)$$

hence becomes a function of the particle circulation; increasing the solids flux in the reactor system leads to a decrease in  $\Delta X$ .

### **2.2 Oxygen carriers for CLC/CLOU**

Substantial research efforts have been devoted to the development and testing of oxygen carrier particles. Oxygen carriers can either be pure materials, such as ores and industrial by-products [45], or manufactured, usually by combining the active metal oxide with some support material in order to increase the mechanical stability [47]. A thorough thermodynamic analysis of different metal oxides [48] showed that  $\text{Fe}_2\text{O}_3/\text{Fe}_3\text{O}_4$ ,  $\text{Cu}_2\text{O}/\text{Cu}$ ,  $\text{Mn}_3\text{O}_4/\text{MnO}$  and  $\text{NiO}/\text{Ni}$

were most suitable for CLC processes using natural gas as fuel. For manufactured oxygen carriers, options for preparation include freeze-granulation [49], spray-drying [50], impregnation [51], co-precipitation [52], spin-flash drying (Paper I) and a few others.

Oxygen carriers can be characterized from a physical, chemical, economical or environmental viewpoint. The ideal oxygen carrier should have:

- A porous structure with a large surface area, thus increasing the accessibility of the reacting gases to the metal oxide;
- High rates of oxidation and reduction. This is necessary in order to minimize the size of the reaction chambers and the amount of needed material;
- High fluidizability and resistance to agglomeration;
- Sufficient mechanical strength, stability in fluidized beds and low tendency of attrition and fragmentation. These features are desirable in order to minimize the production of fines and maximize particle lifetime;
- High melting temperature in oxidized as well as reduced form. Materials become soft when their melting temperature is approached. Operating a CLC system close to the melting temperature of the oxygen carrier may result in agglomeration;
- Capability to convert the fuel entirely to  $\text{CO}_2$  and  $\text{H}_2\text{O}$ , *i.e.* no thermodynamical limitations;
- Low cost with respect to production and raw materials;
- Environmental compatibility and low toxicity.

The choice of oxygen carrier largely depends on the intended application; gaseous fuels, solid fuels and reforming applications all place different demands on the carrier. Solid fuels put more emphasis on low cost and reactivity with syngas. In solid-fuel applications, ash discharge and ash fouling may reduce the lifetime of the carrier, which is why cost is especially important in CLC with solid fuels. Natural minerals provide a low-cost option for oxygen carriers. The feasibility of using minerals as oxygen carriers in CLC has been investigated and demonstrated previously in a number of studies [18,19,20,21,23,26,45,46,53,54,55].

In contrast, natural gas requires high reactivity with methane, but the lifetime of the carrier will not be compromised by ash. This is also reflected in the focus on expensive nickel-based materials for gaseous fuels [16,50,52,56].

An important property of the oxygen carrier is the oxygen ratio, defined as the mass fraction of oxygen available in the oxygen carrier,

$$R_0 = \frac{m_{ox} - m_{red}}{m_{ox}}, \quad (12)$$

where  $m_{ox}$  and  $m_{red}$  are masses of a fully oxidized and a fully reduced sample. A high  $R_0$  is usually considered an advantage since it means that excessive circulation rate of the solid material can be avoided. Table 1 presents  $R_0$  for some commonly investigated metal oxide systems, three of which have been used as carriers in this thesis.

**Table 1. Theoretical  $R_0$  for some metal oxide systems.**

Oxidized form	Reduced form	$R_0$
NiO	Ni	0.21
CuO	Cu <sub>2</sub> O	0.089
Fe <sub>2</sub> TiO <sub>5</sub> ·TiO <sub>2</sub>	FeTiO <sub>3</sub>	0.05
Mn <sub>3</sub> O <sub>4</sub>	MnO	0.075

### 2.2.1 CLOU and Mn-based oxygen carriers

CLOU, chemical-looping with oxygen uncoupling, is closely related to CLC with one crucial difference: gaseous oxygen is released by the oxygen carrier in the FR, according to



The process was proposed in 2005 by Lyngfelt and Mattisson in a patent application [57], but had previously been investigated by Lewis *et al.* [58] using copper oxides. Based on oxides of manganese, copper and cobalt, Mattisson *et al.* proposed three metal oxide systems with oxygen-uncoupling properties [59]. One of these systems was Mn<sub>2</sub>O<sub>3</sub>/Mn<sub>3</sub>O<sub>4</sub>. The pure Mn<sub>2</sub>O<sub>3</sub>/Mn<sub>3</sub>O<sub>4</sub> oxide system has the ability to release gas-phase oxygen but requires temperatures lower than the ones projected for CLC applications. The equilibrium partial pressure of oxygen for Mn<sub>2</sub>O<sub>3</sub>/Mn<sub>3</sub>O<sub>4</sub> is 21% at 877°C, and in a real system, the concentration of oxygen in the AR would be around 5% which implies that oxidation of Mn<sub>3</sub>O<sub>4</sub> to Mn<sub>2</sub>O<sub>3</sub> can occur only below 800°C. However, by combining manganese with Fe, Ni, Si or Mg, limits for these phase transitions become more favorable for CLC [60,61]. The Mn/Fe system has been the topic of several recent investigations [55,62,63] due to its oxygen-release characteristics. Furthermore, the perovskite CaMn<sub>0.875</sub>Ti<sub>0.125</sub>O<sub>3</sub> show promise as a CLOU-carrier [64,65].

The system  $\text{Mn}_3\text{O}_4/\text{MnO}$ , although lacking CLOU properties, has shown favorable oxygen-carrier characteristics [49,66]. In a study by Johansson *et al.* [66], four different Mn based materials were manufactured using zirconia as support. It was found that the reactivity was inversely proportional to the calcining temperature and the crushing strength. When using an Mn ore with only small amounts of iron as oxygen carrier (Paper VI), it is likely that the dominating phases for the Mn ore are  $\text{Mn}_3\text{O}_4$  (oxidized) and  $\text{MnO}$  (reduced).

### 2.2.2 NiO-based oxygen carriers and natural gas as fuel

Nickel-based oxygen carriers have a number of advantages, the most important of which are high melting temperature and high rate of reaction with gaseous fuels.  $R_0$  for Ni/NiO is also relatively high (*cf.* Table 1). On the other hand, nickel is expensive and more toxic than other metals identified as suitable as oxygen carriers.

Nickel oxide and methane (14), and nickel and oxygen (15) react ideally according to:

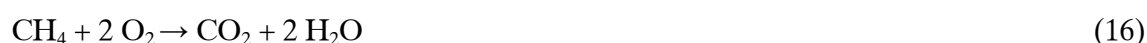


$$\Delta H_{1000^\circ\text{C}} = 133.6 \text{ kJ/mole CH}_4$$



$$\Delta H_{1000^\circ\text{C}} = -468.5 \text{ kJ/mole O}_2$$

The reaction between NiO and methane is endothermic, and consequently there will be a temperature drop in the fuel reactor. When reactions (9) and (10) are combined, the remaining components represent conventional combustion of methane with oxygen:



$$\Delta H_{1000^\circ\text{C}} = -803.4 \text{ kJ/mol CH}_4$$

Oxygen carriers based on nickel cannot completely convert methane to  $\text{H}_2\text{O}$  and  $\text{CO}_2$  [56]; there will be small amounts of CO and  $\text{H}_2$  present in the product gas (Table 2). The amounts of incombustible gases are functions of the temperature in the fuel reactor and can be calculated thermodynamically using minimization of Gibbs free energy. Table 2 shows equilibrium fractions of  $\text{H}_2$  and CO as a function of temperature.

**Table 2. Equilibrium fractions of CO and H<sub>2</sub> during combustion with CH<sub>4</sub> after condensation of H<sub>2</sub>O as calculated with HSC Chemistry 5.1.**

	T (°C)			
	650	750	850	950
CO (%)	0.22	0.40	0.65	0.98
H <sub>2</sub> (%)	0.87	1.02	1.16	1.31

Nickel acts as a catalyst in steam reforming of natural gas:



Through this steam reforming mechanism, nickel contributes to the conversion of the natural gas, which explains why it is beneficial to keep the solids circulation low when operating a chemical-looping combustor with a NiO-based oxygen carrier. The solids circulation determines the difference in particle conversion,  $\Delta X$ , between the AR and the FR. A low circulation rate means that the conversion difference is high, and thus, the particles in the fuel reactor will contain considerable amounts of metallic Ni, *i.e.* sites where steam reforming is catalyzed, thus improving fuel conversion.

### 2.2.3 Ilmenite with solid fuels

The use of ilmenite as oxygen carrier with solid fuels has been the topic of many studies [18,19,20,21,26,46,67]. Oxidation of pure ilmenite can be written



with a standard heat of reaction of  $-444.8$  kJ/mole O<sub>2</sub> at 950°C. Recent studies suggest that ilmenite particles undergo structural change when subjected to the cyclic red-ox reality of CLC [67]. The study found that, due to iron-oxide migration, an Fe<sub>2</sub>O<sub>3</sub>-rich shell has been formed at the surface of the ilmenite along with a TiO<sub>2</sub> enriched core. This would significantly change the thermodynamic properties of ilmenite.  $R_0$  would decrease and the standard heat of reaction for oxidation of magnetite,



is  $-480.4$  kJ/mole O<sub>2</sub> at 950°C. Hence, heat release in the AR would increase.

## 2.3 Lifetime of oxygen carrier

Oxygen-carrier particles are continuously worn down as an effect of operation. In any fluidized-bed process, bed material is exposed to abrasive wear and also, to lesser extent, fragmentation, whereby larger fragments are produced. Wear, or attrition, is caused by

particle-particle interactions and particle-reactor surface interactions, particularly where local velocities are high, *e.g.* around nozzles. Compared to other fluid-bed applications, attrition processes may be more pronounced in a CLC environment, where phase transformation occurring inside the particle may lead to decreased overall or local stress resistance. Attrition resistance is an important characteristic of oxygen carriers. A material that is excessively sensitive to attrition produces a large amount of fines which would increase cost related to (a) pilot/boiler operation and (b) manufacture/procurement of new oxygen carrier.

The rate of attrition, or particle degradation, can be evaluated using a measure called loss of fines,  $L_f$  which is defined as

$$L_f = \frac{\Delta m_{fines}}{\Delta t} \frac{1}{m_I} \text{ (h}^{-1}\text{)}, \quad (20)$$

where  $\Delta m_{fines}$  is the amount of fines produced during a period of time,  $\Delta t$ , and  $m_I$  is the total solids inventory of oxygen carrier in the system.

The lifetime of the oxygen carrier corresponding to the loss of fines can then be calculated approximately as

$$t_{life} = \frac{1}{L_f} \text{ (h)}. \quad (21)$$

An estimation of  $t_{life}$  should preferably be based on long duration of operation using the same batch of particles, *e.g.* hundreds of hours.

An important difference with solid fuels is the formation of ashes, which means that a large mass flow of ash has to be continuously discharged from the combustion of most solid fuels. This ash discharge, and possibly also fouling by ash, is expected to limit the lifetime of the oxygen carrier. Consequently, there is less emphasis on proving a long life-time of the oxygen carriers used with solid fuels.

### 3. Experimental

#### 3.1 Reactor systems

The experimental work presented in this thesis has been carried out in three CLC reactor systems, two of which are operated with gaseous fuel, primarily natural gas, and one which is operated with solid fuel. All three units utilize the concept of interconnected fluidized beds with an air reactor and a fuel reactor, where the gas velocity in the air reactor provides the driving force for particle circulation. Figure 10 shows general representations of the three units; (A) 10 kW unit for gaseous fuels – “Gas-10 kW”; (B) 300 W unit for gaseous fuels; (C) 10 kW unit for solid fuels – “SF-10 kW”.

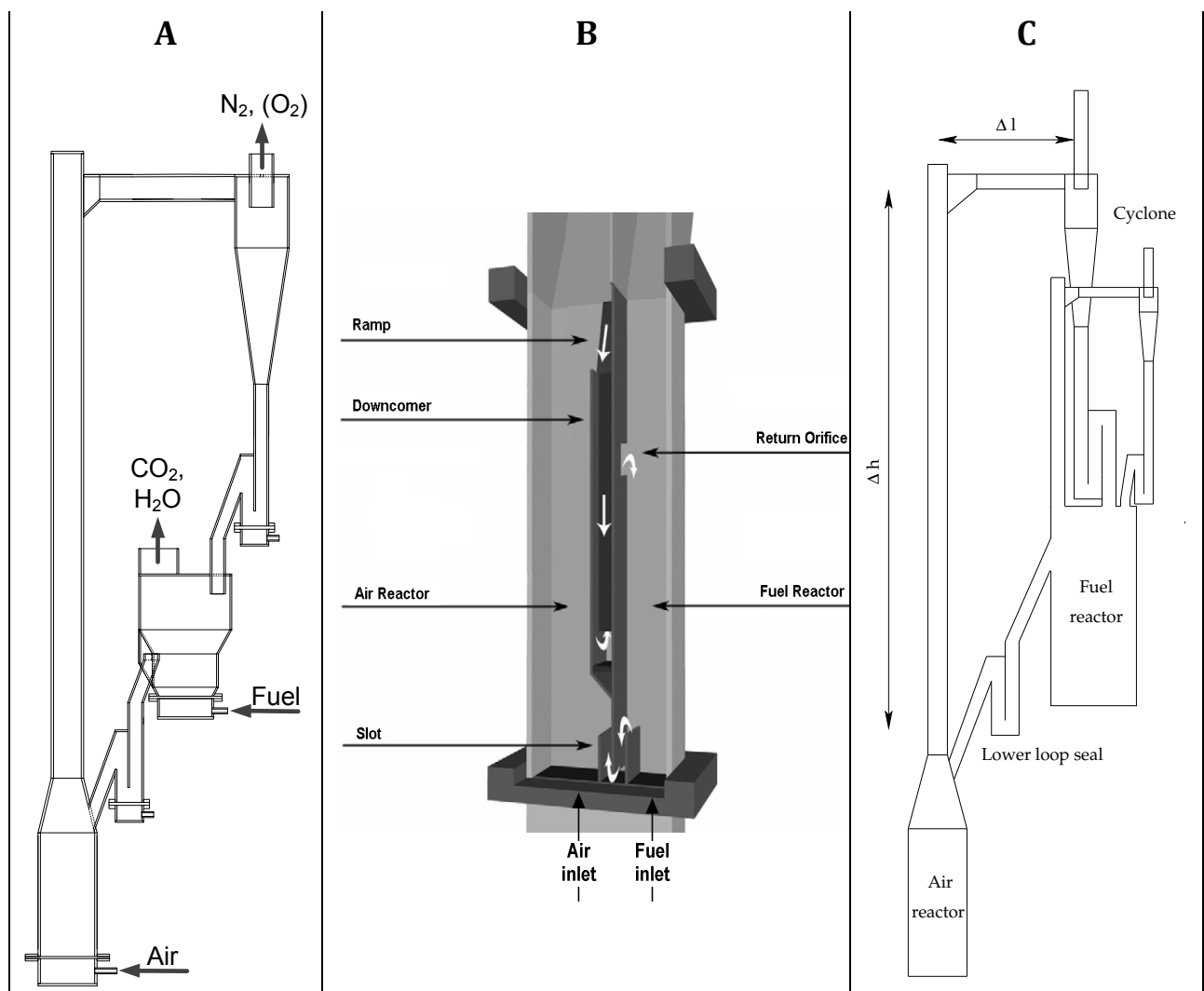


Figure 10. Principal layout of reactor systems; (A) 10 kW unit for gaseous fuels (“Gas-10 kW”); (B) 300 W unit for gaseous fuels; (C) 10 kW unit for solid fuels (“SF-10 kW”).

Separation of particles from the gas flow is achieved by cyclones in the 10 kW units and by simply expanding the cross-section above the air reactor in the 300-W unit (Fig. 10, center). In

both 10 kW units, the bed height in the FR is controlled by an overflow, which means that the bed inventory is fixed, whereas the inventory of the fuel reactor in the smaller unit is determined by (a) the total solids inventory and (b) the height of a water column, through which the pressure difference – and hence the relative bed height – between the air and fuel reactors can be altered. Loop seals are used to prevent gas leaks between the AR and FR.

The FR of SF-10 kW is divided into two principle sections: the low-velocity section (LOVEL) and the carbon stripper (CS). Most reactions occur in the LOVEL, which is fluidized with steam. The CS, fluidized with N<sub>2</sub>, is operated at higher gas velocity than LOVEL. The function of the CS is to return particles to the LOVEL via a recirculation loop, and in this way, increase the residence time of the char.

The superficial velocity used in the reactor system is approximately 0.15 m/s for the reacted gas in the fuel reactors of both 10-kW units and the 300-W unit, assuming a temperature of 850°C, whereas the velocity in the air reactor, after compensating for the oxygen depletion in the combustion air due to reaction, differs between the reactor systems:

- In the 10-kW units, the typical superficial velocity (1000°C and  $\lambda = 1.25$ ) is 3 m/s in the riser and 0.7 m/s in the air reactor;
- In the 300-W unit, the typical velocity (850 °C and  $\lambda = 1.25$ ) is 0.7 m/s in the upper part of the air reactor.

The 300 W unit and SF-10 kW are enclosed in ovens, which makes operation more convenient: the heating is faster and hence the start-up period shorter. The oven is easily opened and requires no removal of insulation, which makes the whole reactor system easily accessible, a feature that (a) facilitates exchange of particle inventory, and (b) means that technical problems can be quickly addressed. This is an obvious advantage in comparison to Gas-10 kW.

### **3.1.1 Construction material for reactor system**

The reactor systems are constructed with a stainless steel called 253 MA. This material is a chromium-nickel steel alloyed with nitrogen and rare earth metals. It contains 11%<sub>mass</sub> Ni and 21%<sub>mass</sub> Cr. Its density is 7800 kg/m<sup>3</sup>, and its thermal expansion is such that it will elongate 1.95% when heated from 30°C to 1000°C. Hence, a total elongation of 4 cm would be experienced by a 2-m tall reactor system, which is the approximate size of the 10 kW units.

253 MA maintains its heat resistant properties by advanced control of micro alloy additions. The use of rare earth metals in combination with silicon gives superior oxidation resistance up to 1100°C. Nitrogen, carbon and a dispersion of rare earth and alkali metal oxides combine to

provide high creep rupture strength. The most suitable operating temperature range is 850-1100°C, because structural changes when used between 600 and 850°C can lead to reduced impact toughness at room temperature.

### 3.1.2 Solids circulation

Solids circulation cannot be directly measured in the units. However, for the 10-kW units, the solids flux can be expressed as a function of the gas velocity and the pressure drop at the top of the riser. According to Johansson *et al.* [68], the following correlation can be used to calculate the net solids flux for a specific unit geometry:

$$G_s = \rho_{exit}(u - u_t) = -\frac{1}{g} \frac{dp}{dh}(u - u_t), \quad (22)$$

where  $u$  is the superficial velocity,  $u_t$  is the terminal velocity of an average sized particle and  $\rho_{exit}$  is the particle density at the riser exit. Since it is not possible to obtain solid samples from the top of the riser,  $u_t$  is based on the average particle size of the fresh material. The applicability of this expression depends on (a) the actual value of  $u_t$  at the top of the riser, (b) accuracy in pressure drop measurement in the upper part of riser, and (c) the ratio of solids externally recirculated to that internally separated at the top of the riser. For both 10-kW units, the solids circulation calculated by equation (22) is believed to give a significant overestimation. Nevertheless, it provides a useful means for comparing particle circulations during the entire test period. In Papers I-II, a circulation index (CI) is obtained by multiplying  $G_s$  with the cross sectional area of the riser and integrating  $dp/dh$  over the entire riser. CI has units kg/min.

For Gas-10 kW, it is possible to calculate the actual circulation by a heat balance over the fuel reactor. Since the reaction in the fuel reactor is endothermic for NiO-based particles, there is a temperature drop which is related to the magnitude of the solids circulation; a low solids flow leads to a sharp temperature decrease and vice versa. This temperature difference was used to estimate the circulation in Papers I and II. A detailed description of the method, including assumptions and simplifications, is presented in Paper II.

For SF-10 kW, a correlation for solids circulation has been established by Markström *et al.* [69]. Here, the average residence time of oxygen carrier particles in the FR,  $\tau_{OC,FR}$ , is determined by making batch tests in the FR with global circulation of solids, and using gas concentrations to study when the reduced particles reach the AR. The solids circulation,  $\dot{m}_{OC}$ , can be obtained as

$$\dot{m}_{OC} = \frac{m_{OC,FR}}{\tau_{OC,FR}}, \quad (23)$$

where  $m_{OC,FR}$  is the solids inventory in the FR. It should be noted that Paper VI uses the residence time in the LOVEL section,  $\tau_{OC} = 0.75\tau_{OC,FR}$ , due to the fact that essentially all reactions occur in the LOVEL since it is fluidized with steam, and the other FR-sections are not.

The solids circulation,  $\dot{m}_{OC}$ , could then be directly correlated to a circulation index (similar to the one described above),

$$CI = \Delta P_{RI} \cdot F_{AR} \cdot \frac{T_{AR} + 273}{273}, \quad (24)$$

where  $\Delta P$  is the pressure drop in the riser, and  $F_{AR}$  and  $T_{AR}$  are flow and temperature in the AR. In this work, a linear relationship between  $\dot{m}_{OC}$  and CI was found for SF-10kW, which could be expressed as,

$$\dot{m}_{OC} = \frac{m_{OC,FR}}{1178} CI, \quad (25)$$

In Paper III, the temperature difference between the air and fuel reactors in the 300-W unit is used as a measure of circulation. However, it is an approximate method that only provides a relative measure of circulation.

### 3.1.3 Gas leakage

Gas leakages between the air and fuel reactors have to be minimized. Leakages from the fuel reactor to the air reactor would lead to CO<sub>2</sub> escaping into the atmosphere and would thus decrease carbon capture efficiency, whereas a leakage of air to the fuel reactor would dilute the CO<sub>2</sub> stream with nitrogen, which might result in extra costs for CO<sub>2</sub> purification. The presence of loop seals between the AR and FR is an effective way of minimizing gas leakages. Leakages of gas between the AR and FR are very small in the 10-kW units. In fact, they are below the detection limit. In the 300-W unit, however, there are leakages in both directions. The extent of these leakages was investigated in Paper III and it was shown that the leakage from the fuel to the air reactor is about 5% of the added carbon, whereas the leakage flow in the opposite direction is much smaller, 0-0.2% of the added air, which could oxidize a maximum of 0.2% of the added fuel.

## 3.2 Fuels

### 3.2.1 Gaseous fuel

The fuel used in the experiments in Papers I-III was natural gas, which is composed of approximately 90% methane, 6% ethane, 3% higher hydrocarbons, and 1% N<sub>2</sub> and CO<sub>2</sub>. The lower heating value of the fuel is 39.6 MJ/m<sub>n</sub><sup>3</sup>. The fuel load is per default reported as the fuel power (e.g. 10 kW), which is defined on thermal basis as the product of the lower heating value and the volumetric flow (normalized at 0.1 MPa, 0°C) according to

$$P_{fuel} = H_i \dot{V}_{fuel} . \quad (26)$$

### 3.2.2 Solid fuel

Table 3 shows some properties of the fuels used. In Paper IV, 5 devolatilized fuels are used in order to obtain char reactivity and the conversion of syngas from char gasification. During continuous experiments, two fuels were used; petroleum coke, “Pet coke III” (Papers V and VI) and a bituminous coal, “Colombian” (Paper VI).

**Table 3. Fuel specification with proximate analysis. The top five fuels were used in batch experiments. “Pet coke III” and “Colombian” were used in continuous testing.**

Fuel name	Type	Origin	Devolatilized	Proximate analysis			
				M (%)	A (%)	V (%)	C-fix (%)
RSA	Bituminous coal	South Africa	Yes	4.3	22.4	2.8	70.6
Cerrejón	Bituminous coal	Colombia	Yes	2.3	18.4	11.6	67.7
Colombian	Bituminous coal	Colombia	Yes	2.7	6.2	29.1	62
Met coke	Metallurgical coke	SSAB, Sweden	No	0.3	10.9	0.6	88.2
Pet coke dev.	Petroleum coke	Mexico	Yes	2.3	6.4	2.5	88.9
Pet coke III	Petroleum coke	Mexico	No	1.1	3.9	11.6	83.3

**M: moisture; A: ash; V: volatile matter; C: fixed carbon.**

For solid fuels, fuel power is defined on mass basis,

$$P_{fuel} = H_i \dot{m}_{fuel} , \quad (27)$$

meaning that also  $H_i$  is defined on mass basis.

## 3.3 Oxygen carriers

Oxygen carriers used in combination with gaseous fuels were all based on nickel, whereas natural ores were used with solid fuels. The choice of oxygen carrier depends on the application and has been discussed in the previous chapter.

Minimum fluidization and terminal velocities (Table 4) were calculated according to relations by Kunii and Levenspiel [70]. The average particle diameters are calculated from the particle size distribution of fresh oxygen carriers.

**Table 4. Terminal and minimum fluidization velocities for the particles used in the work. For Ni-based particles,  $u_t$  is calculated for air at 1000°C and  $u_{mf}$  is calculated for a mixture of CO<sub>2</sub> and steam at a ratio of 1:2, corresponding to full oxidation of methane, at 850°C. For the ores,  $u_t$  is calculated for air at 900°C and  $u_{mf}$  is calculated for H<sub>2</sub>O, 970°C, due to different conditions in the two reactor systems.**

Particle	$\bar{d}_p$ (μm)	$u_t$ (m/s)	$u_{mf}$ (m/s)
N-IFP	130	0.70	0.015
N-VITO	135	0.65	0.010
N-VITOMg	135	0.60	0.010
N-CSIC	180	0.70	0.015
Ilmenite	171	0.85	0.025
Mn ore	152	0.62	0.017

### 3.3.1 Oxygen carriers used in experiments with gaseous fuels

All particles used in the experiments with gas were manufactured using a combination of active and support materials (Table 5). Four different NiO-based oxygen carriers were used in the experiments: one particle produced by spin-flash drying (N-IFP, Paper I), two spray-dried particles (N-VITO and N-VITOMg, Paper II and III), and one impregnated particle (N-CSIC, Paper III). Some important characteristics of the oxygen carriers used in the experiments are summarized in Table 5. Apparent density is measured on particles sized 125-180 μm and calculated assuming a void between particles of 37%. The crushing strength is measured on particles of size 180-212 μm. The GRACE particle [71,72], which was used in CLC operation in Gas-10 kW for more than 100 h with very high conversion of fuel [73], has been included for comparison.

**Table 5. Characteristics of the oxygen carriers used in the experiments and the GRACE particle.**

Denotation in thesis	Active material	Fraction of active material (wt-%)	Support material	Production method	Crushing strength (N)	Apparent density (kg/m <sup>3</sup> )	Manufacturer
N-IFP	NiO	60	NiAl <sub>2</sub> O <sub>4</sub>	Spin-flash drying	5.3	4400	IFP
N-VITO	NiO	40	NiAl <sub>2</sub> O <sub>4</sub>	Spray-drying	2.3	3600	VITO
N-VITOMg	NiO	40	NiAl <sub>2</sub> O <sub>4</sub> (~42%) + MgAl <sub>2</sub> O <sub>4</sub> (~18%)*	Spray-drying	2.0	3250	VITO
N-CSIC	NiO	18	α-Al <sub>2</sub> O <sub>3</sub>	Hot impregnation	4.8	2340	CSIC
GRACE	NiO	40	NiAl <sub>2</sub> O <sub>4</sub>	Freeze-granulation	2.5	3800	

\*assuming that all added MgO reacted with Al<sub>2</sub>O<sub>3</sub>.

It is important to point out that, unlike the GRACE particle, the IFP- and VITO-particles were prepared by commercial – *i.e.* less expensive – production methods. Furthermore, in the case of the VITO-particles, the starting materials used were commercially available materials, and not high-purity substances. N-CSIC is an impregnated oxygen carrier that was used in a mixed batch of oxygen carriers in one test in the 300-W unit in order to improve the methane conversion.

SEM images of fresh particles (*i.e.* particles not subjected to CLC) can be seen in Fig. 11. The physical appearance of N-VITOMg (not shown) is very similar to that of N-VITO.

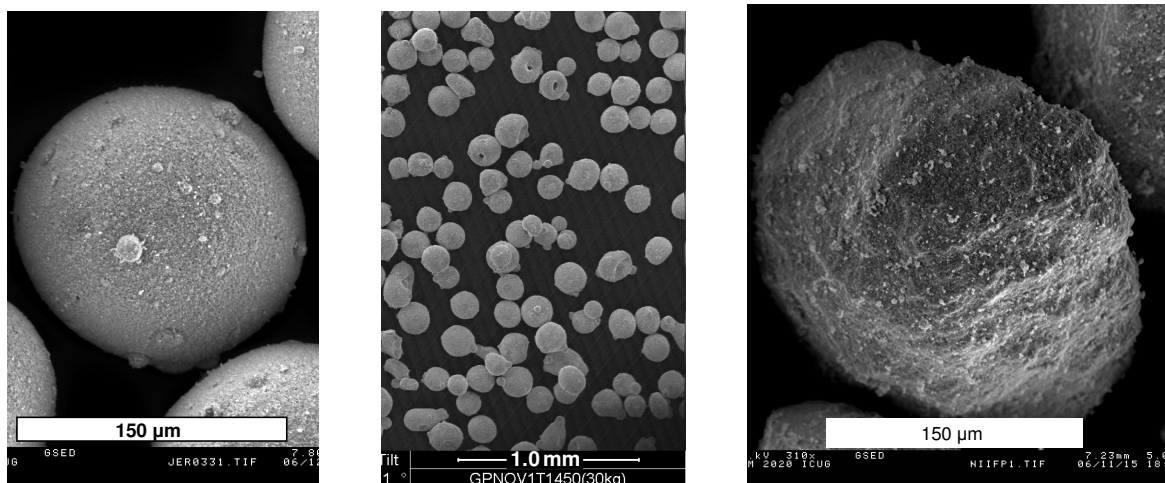


Figure 11. SEM images of fresh N-VITO (left and center) and fresh N-IFP (right).

### 3.3.2 Oxygen carriers used in solid-fuel experiments

Three oxygen carriers based on natural minerals were used in this work,

- A. Ilmenite (Papers IV-VI)
- B. Ilmenite + limestone (Paper V)
- C. Mn ore (Paper VI)

As stated above, primarily low-cost oxygen carriers are studied for solid fuels, where ash discharge and fouling may limit the lifetime of a carrier. Natural minerals provide a low-cost option for oxygen carriers.

Ilmenite,  $\text{FeTiO}_3$  (reduced form), is a weakly magnetic iron-titanium mineral which is produced in large quantities worldwide. The ilmenite used in this study has 94.3% purity. The same material – although not the same batch of particles – has previously been used in the SF-10 kW for approximately 90 h of operation [18,19,20,21]. Advantages as oxygen carrier are low cost, no thermodynamical limitations, high melting point, high mechanical strength and stability in fluidized beds, reasonable rates of oxidation and reduction, and no health or environmental issues.

Manganese ore is also mined in large quantities and would be a low-cost material, although more expensive than ilmenite. It has paramagnetic properties, which could be advantageous in solid-fuel CLC applications since it enables separation from ash of elutriated particles. Elemental composition may vary significantly between ores. Using a Slovakian manganese ore, Rydén *et al.* [55] reported experiments showing some oxygen uncoupling but raising concerns regarding mechanical stability. The batch of manganese ore used in the present experiments originates from Brazil. It was ground at Höganäs, Sweden and sieved to the desired size fraction, 70-300  $\mu\text{m}$ , at Chalmers.

Ilmenite and Mn ore have similar properties as oxygen carriers, although there is a difference in crushing strength (Table 6), which could explain why Mn ore is more sensitive to attrition.  $R_0$  was determined experimentally. Fresh particles of size 180-212  $\mu\text{m}$  were used for determining crushing strength. SEM images of fresh and used particles are shown in Fig. 12.

**Table 6. Characteristics of the oxygen carriers used in the experiments.**

Property	Units	Ilmenite	Mn ore
$\rho_{\text{apparent}}$	$\text{kg/m}^3$	3700	3200
Crushing strength	N	3.85	1.25
$R_0$	-	0.039	0.030

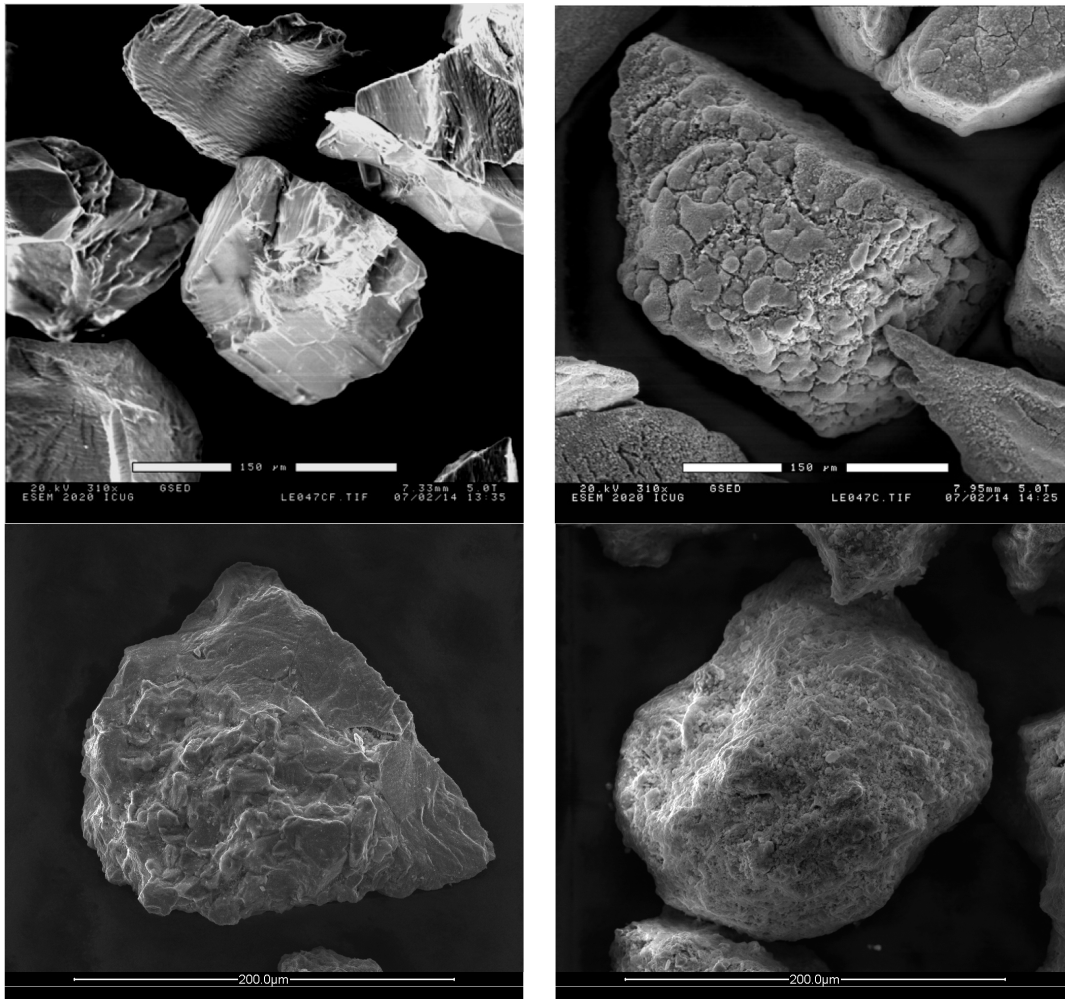


Figure 12. SEM images. Top left, fresh ilmenite; top right, ilmenite used in batch testing; bottom left, fresh Mn ore; bottom right, Mn ore used in batch testing. Ilmenite images from [74]. The white bar is 150  $\mu\text{m}$  for ilmenite and 200  $\mu\text{m}$  for Mn ore.

### ***3.4 Gas measurements, definitions and analysis***

Online gas analysis allows measurement of the oxygen, carbon dioxide and carbon monoxide concentrations from both reactors after condensation of water. Additionally, methane is measured in flue gas from the FR. In solid-fuel experiments,  $\text{H}_2$  and  $\text{SO}_2$  are also measured in the FR flue gas. In gaseous-fuel experiments, hydrogen was measured only intermittently with a gas chromatograph.

#### **3.4.1 Data evaluation with gaseous fuel**

Carbon monoxide, methane, hydrogen and carbon dioxide concentrations are presented as fraction of total carbon from the fuel reactor according to

$$f_i = \frac{x_i}{x_{CO_2} + x_{CO} + x_{CH_4}}, \quad (28)$$

where  $i$  represents  $CO_2$ ,  $CO$ ,  $CH_4$  and  $H_2$ , and  $x$  is the volume fraction of the substance indicated by the sub-script in dry exit gas from the fuel reactor. The measured concentrations of  $CO$ ,  $CO_2$ ,  $CH_4$  and  $H_2$  are somewhat lower due to dilution with nitrogen from the loop seals.

The combustion efficiency is calculated according to

$$\eta_{comb} = 1 - \frac{H_{i,CO} \dot{V}_{CO} + H_{i,CH_4} \dot{V}_{CH_4} + H_{i,H_2} \dot{V}_{H_2}}{H_{i,fuel} \dot{V}_{fuel}}, \quad (29)$$

where  $H_i$  is the lower heating value and  $\dot{V}$  is the volumetric flow ( $m_n^3/s$ ).

### 3.4.2 Data evaluation with solid fuel

Compared to gaseous fuels, evaluation of data is more complex for solid fuels since fuel conversion has to be addressed both as (a) char conversion to gas, and (b) gas conversion to  $CO_2$ . Gaseous species produced in the FR are either volatile compounds or products of char gasification. Volatiles include mainly  $CH_4$ ,  $H_2$ ,  $CO$  and  $CO_2$ . Higher hydrocarbons are also present to smaller extent, but these are not measured.

It is necessary to know the size of the flows of the different gases from the FR. Since only concentrations, and not flows, are measured downstream of FR, determination of these flows is made possible by the presence of a known flow of  $N_2$ , used to fluidize certain parts of the FR. Hence, the total volumetric flow from the fuel reactor can be calculated through,

$$F_{total,FR} = \frac{F_{N_2}}{x_{N_2}} = \frac{F_{N_2}}{1 - (x_{CO_2} + x_{CO} + x_{CH_4} + x_{H_2} + x_{H_2S} + x_{SO_2})}, \quad (30)$$

where  $F_i$  ( $L_n/min$ ) denotes flow of gas  $i$ , and  $x_i$  is the volume fraction of gas  $i$ . Flows of individual gas components can then be calculated by

$$F_i = x_i \cdot F_{total,FR}. \quad (31)$$

The total concentration of sulfur containing gases is calculated from the fuel composition and the total concentration of carbon containing gases at the outlet of the fuel reactor assuming (a) that the S/C ratio is the same in the fresh fuel as in the gas leaving the fuel reactor, and (b) that no other sulfur species than  $SO_2$  and  $H_2S$  are formed. The concentration of  $H_2S$  is then deduced from the  $SO_2$  concentration.

Fuel that enters the FR can follow one of three routes: (a) conversion to gas in the FR, which is the desired case, (b) conversion in the AR – some char will inevitably follow the flow of oxygen carrier to the AR where it burns to CO<sub>2</sub>, or (c) exit the FR via the chimney as unconverted char. The fuel fraction that is converted to gas in the entire system, *i.e.* in both FR and AR, can be written as

$$\eta_{SF} = \frac{F_{CO_2,AR} + F_{CO_2,FR} + F_{CO,FR} + F_{CH_4,FR}}{\dot{m}_{C,fuel}} \frac{M_C}{V_n} \quad (32)$$

where  $\dot{m}_{C,fuel}$  (g/min) is the mass flow of carbon in fuel to the FR,  $M_C$  (g/mole) is the molar mass of carbon and  $V_n$  is the molar volume of an ideal gas normalized at 0.1 MPa and 0°C, 22.7 L<sub>n</sub>/mole.

The oxygen demand describes the fraction of oxygen lacking to achieve complete combustion of the gas produced in the FR,

$$\Omega_{OD} = \frac{0.5x_{CO} + 2x_{CH_4} + 0.5x_{H_2} + 1.5x_{H_2S}}{\Phi_O(x_{CO_2} + x_{CO} + x_{CH_4})}, \quad (33)$$

where  $\Phi_0$  is the molar ratio [ $n_{O_2}$  required for combustion/kg fuel] / [ $n_C$ /kg fuel]. Consequently,  $\Omega_{OD}$  is a measure of the gas combustion efficiency in the FR. Pet coke is rich in sulfur, which is why it is important to account for sulfur species.

The carbon capture efficiency,  $\eta_{CC}$ , is the ratio of the carbon converted to gas in the FR to the total flow of gaseous carbon from the reactor system. This efficiency reflects unconverted char reaching the air-reactor and being burnt to CO<sub>2</sub>.

$$\eta_{CC} = \frac{F_{CO_2,FR} + F_{CO,FR} + F_{CH_4,FR}}{F_{CO_2,AR} + F_{CO_2,FR} + F_{CO,FR} + F_{CH_4,FR}}, \quad (34)$$

Another way of expressing the process performance is by the gasification efficiency,

$$\eta_{gas} = \frac{(F_{CO_2,FR} + F_{CO,FR} + F_{CH_4,FR}) \cdot M_C / V_n - \dot{m}_{C,vol}}{\dot{m}_{C,fuel} - \dot{m}_{C,vol}}, \quad (35)$$

where  $\dot{m}_{C,fuel}$  (g/min) is the mass flow of carbon contained in the fuel flow, and  $\dot{m}_{C,vol}$  (g/min) is the mass flow of carbon in the volatile compounds.

In normal combustion processes, the amount of excess oxygen is described by the air-to-fuel ratio. In CLC, oxygen availability in the FR can be expressed by the OC/fuel ratio, which is the

amount of oxygen supplied by the oxygen carrier divided by the oxygen required for complete oxidation of the gas produced in the FR,

$$OC / fuel = \frac{\dot{m}_{OC} \cdot R_0 \cdot 1000 / M_{O_2} \cdot V_n}{\Phi_o (F_{CO_2,FR} + F_{CO,FR} + F_{CH_4,FR})}, \quad (36)$$

where  $M_{O_2}$  (g/mole) is the molar mass of oxygen and  $R_0$  is the mass ratio of available oxygen in the oxygen carrier.

Batch tests are evaluated using  $\Omega_{OD}$  and the instantaneous rate of fuel conversion,  $k_{inst}$ ,

$$k_{inst}(t) = \frac{\dot{m}_C(t)}{m_{C,FR}(t)}, \quad (37)$$

where  $m_{C,FR}(t)$  is the amount of non-reacted carbon present in the fuel reactor at time  $t$ , and  $\dot{m}_C(t)$  is the mass flow of gaseous carbon, *i.e.* carbon converted to CO, CO<sub>2</sub> and CH<sub>4</sub>.

## 4. Results

Experiments have been performed in three chemical-looping combustors. The main results of the investigations in this thesis are given below.

### 4.1 Natural gas experiments

In Papers I and II, the Gas-10 kW is used to study the effects of long-term CLC operation on oxygen-carrier particles. In Paper III, the 300 W unit is used to evaluate two spray-dried particles, individually and mixed, with the purpose of finding the optimally performing batch with respect to fuel conversion.

#### 4.1.1 Papers I and II: long-term tests in Gas-10 kW

Paper I evaluates the performance of N-IFP and Paper II that of N-VITO and N-VITOMg. Prior to the experiments accounted for in Papers I and II, the Gas-10 kW unit had been used for testing of the GRACE-particle, and the results from those tests will be used here for comparison.

##### *Duration of fuel operation*

The GRACE-particle was tested for 105 h; N-IFP was subjected to 160 h of operation; and the VITO-particles were used for > 1000 h of operation with fuel in the 10-kW reactor system.

Of the 1016 h of fuel operation achieved with the VITO-particles, the first 405 h were accomplished using a single batch of N-VITO. The last 611 h were achieved using a 50/50-mass-mixture of (i) N-VITO-particles used for 405 h, and (ii) fresh N-VITOMg. Thus, at the conclusion of the test series, approximately half of the particles in the reactor system had been subjected to > 1000 h of chemical-looping combustion, whereas the other half had been used for 611 h. The idea behind using a mixed oxide system of these particular oxygen carriers originated from findings that the addition of MgO or the use of  $\text{MgAl}_2\text{O}_4$  has a significant effect on the methane conversion [75]. However, the oxygen transport capacity is relatively low for this type of oxygen carrier, especially at lower temperatures. Hence, the mixture of these two particles may result in a more optimal system, in comparison to using either of the oxygen carriers alone.

##### *Fuel conversion*

Generally, conversion of the natural gas improves with increasing fuel-reactor temperature and decreasing rate of particle circulation. This has been observed for all particle batches. For the GRACE-particle and N-IFP, the fraction of CO exiting the fuel reactor followed the

thermodynamical equilibrium quite closely, whereas for the VITO-particles, CO fractions were slightly above equilibrium.

Table 7 shows performance of the different particles at  $T_{FR} = 800-850^{\circ}\text{C}$ . Here, the hydrogen fraction is obtained assuming that the water-gas shift reaction,



is at equilibrium and that the ratio  $\text{H}_2\text{O}/\text{CO}_2 = 1.85$ , which is true when oxidation of the natural gas is complete, since the H/C-ratio is 3.7. The equilibrium constant,  $K$ , is obtained from HSC Chemistry 5.1.

**Table 7. Performance of oxygen carriers used in Gas-10 kW at  $T_{FR} = 800-850^{\circ}\text{C}$ .**

	$P_{fuel}$ (kW)	$T_{FR}$ ( $^{\circ}\text{C}$ )	$K$	$f_{CH_4}$ (%)	$f_{CO}$ (%)	$f_{CO_2}$ (%)	$f_{H_2}$ (%)	$\eta_{comb}$ (%)
<b>GRACE</b>	10	800	1.06	0.15	0.4	99.45	0.78	99.5
<b>N-IFP</b>	11	850	0.89	0.35	0.65	99.0	1.07	99.1
<b>N-VITO</b>	10	840	0.92	0.9	1	98.1	1.71	98.2
<b>N-VITO &amp; N-VITOMg</b>	10	850	0.89	0.23	1.26	98.5	2.08	98.7

For the GRACE-particle, the highest fuel conversion was obtained at  $800^{\circ}\text{C}$ . At this temperature, the optimum solids circulation was reached.

During stable operation, the fuel-reactor temperature is tightly linked to the solids circulation. When the temperature in the air reactor is  $1000^{\circ}\text{C}$ , which is the normally used temperature, the fuel-reactor temperature is usually  $800-900^{\circ}\text{C}$ . It is possible to investigate lower temperatures at start-up, and also by changing the temperature of the incoming particles, *i.e.* by decreasing the temperature in the air reactor. This latter option, however, is not normally used, since it requires substantial cooling flows to remove heat evolved in the exothermic reaction.

Operation with the GRACE-particle below  $800^{\circ}\text{C}$  was reported to result in an increase of CO, but this might have been an effect of low circulation, *i.e.* insufficient supply of oxygen [71]. With N-IFP, temperatures as low as  $660^{\circ}\text{C}$  were investigated, and it was found that CO followed the equilibrium. Using the mixed VITO-batch, the fuel reactor was operated  $< 650^{\circ}\text{C}$  with little  $\text{CH}_4$  in the fuel-reactor exit gas, but a lot of CO. As in the case with the GRACE-particle, this might have been an effect of low circulation.

### *Loss of fines*

The loss of fines was used to calculate the expected particle life time for the GRACE-particle, the IFP-particle, and the mixed VITO-batch. The expected lifetimes for the GRACE- and IFP-particles were 40000 h and 4500 h, respectively. A lot of fines were produced during operation with N-IFP, which was evident both during handling of the particles and by studying the mass balance. Nevertheless, it is possible that a fraction of the fines may have escaped through the filter bags, where elutriated material from the air reactor is collected. Prior to the VITO-runs, the filter bags were replaced with new ones that had lower cut-off diameter. The collection and handling of fines produced in the VITO-runs followed a meticulous procedure, and it is believed that the calculated expected lifetime, 33000 h, is a reliable estimation as far as mechanical degradation is concerned.

### *Agglomeration*

Sintering of particles is a complex process which is influenced primarily by temperature and chemical environment [76]. Gas velocity and mixing conditions in the fuel reactor also affects sintering behaviour of particles. A low velocity implies more physical contact between particles.

The GRACE-particle showed no signs of agglomeration during operation in the Gas-10 kW. N-IFP agglomerated during sub-stoichiometric ( $\lambda = 0.8$ ) operation. The operation with N-VITO resulted in the formation of agglomerates on a few occasions. Massive agglomeration occurred when the fuel feed was unintentionally decreased.

### *Reactivity and mechanical strength*

Similar observations were made for the GRACE and VITO-particles concerning mechanical strength: a slight increase was observed as an effect of operation. The reactivity of the GRACE- and IFP-particles did not change during operation, whereas the reactivity for the N-VITO and the mixed VITO-batch actually increased during an initial period of time (approximately 50 h).

### *Particle conversion and circulation*

For N-IFP, the solids circulation was calculated to 2-3 kg/min at 11 kW, which would correspond to  $\Delta X \approx 0.2$ .

For the mixed VITO-batch, the solids circulation was calculated to 2-4 kg/min at 10 kW. This circulation was categorized as “moderate” to “high”, and the corresponding  $\Delta X = 0.14-0.27$ . At

low circulation, the FR bed temperature was slowly falling, and therefore, the solids circulation could not be established using the method based on a heat balance over the fuel reactor.

In order to obtain the particle conversion at low circulation, the fuel feed was cut and replaced with air following an experiment at low circulation, while simultaneously, fluidization of the loop seals was terminated, which effectively stopped the circulation of particles. Hence the amount of oxygen needed for complete particle oxidation was obtained, and  $X_{FR}$  could be calculated, which, combined with a knowledge of  $X_{AR}$  (0.98), resulted in  $\Delta X = 0.4$ . A more detailed description of the procedure is given in Paper II.

#### **4.1.2 Paper III: comparison of oxygen carriers**

Spray-dried particles were investigated in a continuous 300-W reactor system. An attempt to optimize the oxygen-carrier performance by mixing two different spray-dried Ni-particles was conducted. Here, the reference particle, N-VITO, was combined with N-VITOMg. The former had favorable oxygen-transport capability while the latter had very good methane-conversion characteristics, as described earlier.

Prior to the experiments carried out in the 300-W reactor system, smaller batches of particles were tested batch-wise in a laboratory reactor. These reactivity investigations were conducted in a fluidized-bed reactor of quartz, and the two spray-dried particles were evaluated individually and mixed. The investigations indicated that mixing of the two oxygen-carrier particles can be beneficial for fuel conversion.

The findings from the batch experiments were evaluated in a 300-W chemical-looping combustor at three temperatures; 750°C, 850°C and 950°C. In general, fuel conversion increased, as expected, with (a) decreased circulation, and (b) increased fuel-reactor temperature. The operation with N-VITO was somewhat unstable, and the fuel conversion was unsatisfactory at  $T_{FR} = 750^\circ\text{C}$ , but high at the higher temperatures. With the mixture of the two spray-dried particles, operation was stable and, in comparison to the operation with only N-VITO, fuel conversion improved at all three temperatures, especially at 750°C. At low circulation, the fraction of unconverted methane was  $< 0.1\%$  both at 850°C and 950°C.

Moreover, a third, NiO-based impregnated oxygen carrier was introduced into the mixture in order to improve the methane conversion even further. This particle, composed of 18% mass NiO on  $\alpha\text{-Al}_2\text{O}_3$ , was prepared by CSIC in Spain [77]. Excellent conversion of the fuel was obtained at relatively high circulation with this three-particle mixture.

## **4.2 Solid fuel experiments**

Paper IV concerns batch tests of five solid fuels using ilmenite as oxygen carrier, and Papers V and VI deals with continuous tests that are aimed at investigating the use of different oxygen carriers based on natural minerals, as well as the effect of different fuel feeding configurations.

### **4.2.1 Paper IV: batch tests in SF-10 kW**

Paper IV explores (a) the rate of char gasification, *i.e.* char conversion to syngas, and (b) the extent of conversion of syngas from char gasification, expressed as oxygen demand.

Gas conversion in previous continuous testing had left room for improvement. It had been shown that the major part of the reducing gases exiting the FR originated from volatiles [20]. The reason for this was poor contact between volatiles and oxygen carrier, which was an effect of the fuel feeding configuration. Therefore, the fuels used in the experiments were primarily devolatilized.

Batches of 20-25 g were fed to the fuel reactor at  $T_{FR} = 940^{\circ}\text{C}$ ,  $970^{\circ}\text{C}$ ,  $1000^{\circ}\text{C}$ , and  $1030^{\circ}\text{C}$ . The aim of the tests was to determine vital parameters for fuel conversion. It was possible to determine (a) oxygen demand associated with syngas from char gasification as well as (b) kinetics of char conversion to gas. Instantaneous rates of char conversion to gas were found to be temperature dependent, as expected. The reaction rate constant for char conversion was found to increase with a factor 1.6 - 3.2 between  $970^{\circ}\text{C}$  and  $1030^{\circ}\text{C}$ . The minimum oxygen demand, assumed to be the same as the oxygen demand for syngas from char gasification, was found to be 4-5% for pet coke and met coke, and 6-11% for the bituminous fuels.

### **4.2.2 Papers V and VI: continuous tests in SF-10 kW**

In Papers V and VI, continuous tests are aimed at investigating properties of different oxygen carriers based on natural minerals:

- A. Ilmenite (Papers V-VI),
- B. Ilmenite + limestone (Paper V),
- C. Mn ore (Paper VI).

An evaluation of above-bed versus in-bed fuel feed is carried out in Paper VI.

#### *General observations*

Effect of fuel type. The bituminous coal is more reactive than the pet coke, possibly due to higher porosity. This is manifested as higher gasification efficiency and higher  $\text{CO}_2$  capture. The gas conversion, however, is not as high for the bituminous coal as for the pet coke, due to

the high amount of volatiles, which – even with the new, improved fuel feed – are only partially oxidized.

Effect of circulation. The global solids circulation controls  $\tau_{OC}$ , which in turn is strongly correlated to the char residence time. Increasing the residence time means that there is more time for the char to gasify. The CO<sub>2</sub> capture and the extent of gasification are clearly increased by increasing the residence time when pet coke is used as fuel.

Effect of temperature. The FR temperature was shown to be a determining variable for the performance of the process. Increasing the temperatures leads to increased rate of gasification and thus increased carbon capture.

The OC/fuel ratio was between 1 and 2. If the ratio gets too low (close to 1), the performance of the process worsened due to insufficient oxygen availability and slower gasification due to generation of high amounts of CO and H<sub>2</sub>, which are gasification inhibitors.

$\Omega_{OC}$  without volatiles. The oxygen demand after stopping of the fuel feed with bituminous coal, fell as low as 6%, indicating a low oxygen demand for conversion of syngas from char gasification.

#### *Effect of limestone addition to ilmenite (Paper V)*

At 950°C limestone addition led to improved gas conversion, with a decrease in oxygen demand from 0.33 to 0.24. However, this behavior was not observed at 1000°C. The improvement seen at 950°C was explained by the effect of limestone on the water-gas shift equilibrium, whereby CO was shifted to H<sub>2</sub>. Since ilmenite reacts faster with hydrogen than CO, the overall effect was to increase the reaction rate and consequently more H<sub>2</sub>O and CO<sub>2</sub> was produced. Furthermore, likely due to the gasification-inhibiting behavior of CO and H<sub>2</sub>, the rate of char conversion was improved with the limestone addition.

The oxygen transfer that could be carried out by sulfated limestone was estimated to be negligible and the improvement in the efficiency of the process is explained by the effect of limestone upon the water-gas shift equilibrium and subsequent reaction with ilmenite as oxygen-carrier.

Thus, the use of some limestone in the process as additive increases the rate of char gasification and improves gas conversion, because the lime catalyzes the water-gas shift reaction.

#### *Fuel feed comparison (Paper VI)*

The in-bed fuel feed has a substantial influence on gas conversion. Gas conversion to CO<sub>2</sub> increases, mainly due to improved contact between oxygen carrier and volatiles. No effect on

gasification is observed, neither is it expected. The in-bed fuel feed, although an improvement compared to the old feeding configuration, is still not optimal and can be further improved, which would promote gas/solids contact and, consequently, gas conversion.

*Mn ore as oxygen carrier (Paper VI)*

In general, both the char gasification rate and the gas conversion are improved when using Mn-ore in comparison to ilmenite. 10.5 h of fuel operation were accomplished with manganese ore as oxygen carrier during two days of operation (Fig. 13). The fuel flow corresponds to 5.9 kW except between 6.6 h < t < 9.6 h, where the flow was reduced to 4 kW.  $\Omega_{OD}$  in the figure includes  $H_2S$ . If  $H_2S$  is excluded, the oxygen demand is as low as 10%, which can be compared to the lowest value found for ilmenite, 18%.

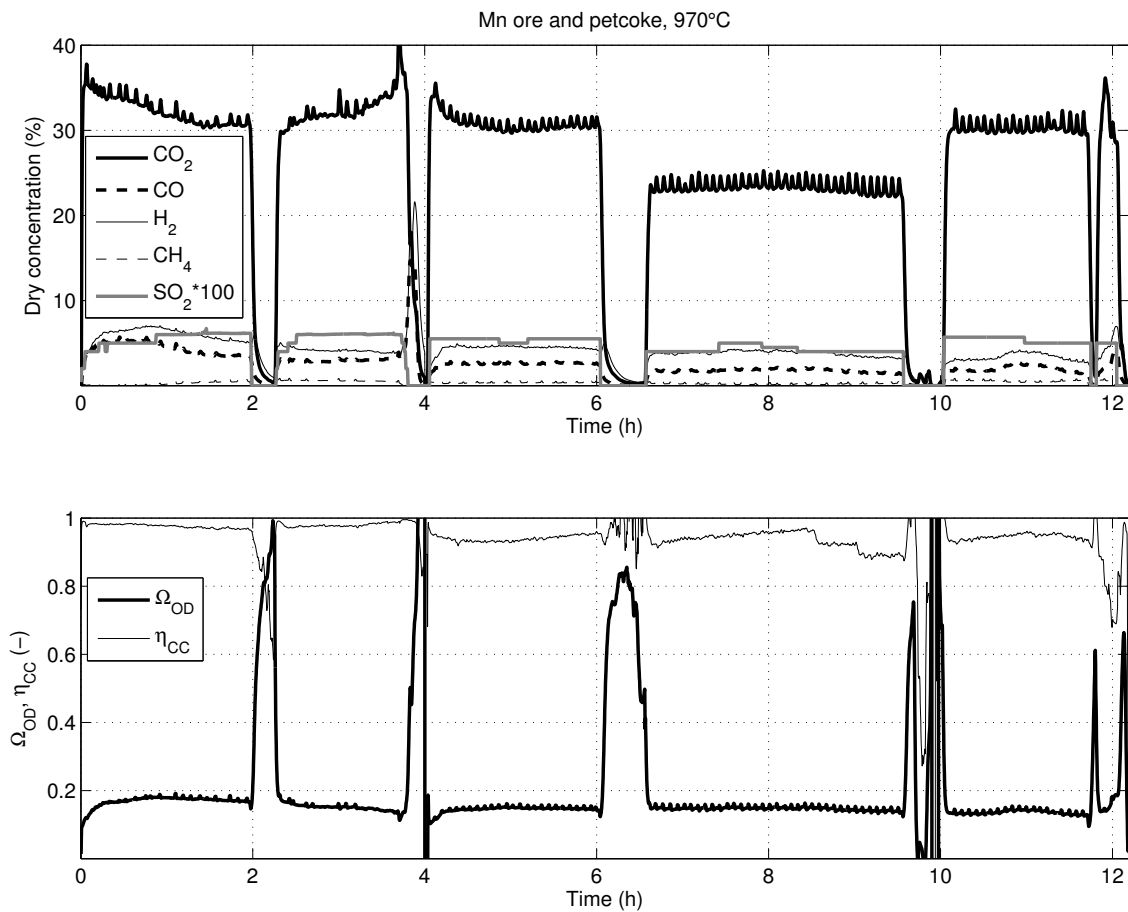


**Figure 13. Manganese ore with pet coke as fuel,  $T_{FR} = 970^{\circ}C$ . Top: dry concentrations of carbon-containing gases and  $H_2$ . Bottom: oxygen demand and carbon capture efficiency. The recurring  $CO_2$  peaks correspond to knocks on the fuel chute.**

Compared to operation with ilmenite, the char gasification rate is profoundly improved, as can be seen from the carbon loss to the AR, which is reduced to 2-6% compared to around 30% for ilmenite.

The mechanical stability of the Mn ore as oxygen carrier in CLC conditions seems to be poor. Using the manganese ore, the fines-production rate,  $L_f \approx 1.6\%/h$ , which is much higher than what has been observed during operation with ilmenite.

#### *CLOU effect*

Laboratory tests with the Mn ore that had been used in the continuous experiments showed a small CLOU effect – the concentration of  $O_2$  was 0.1% on dry basis. During the continuous tests, it was not possible to verify any release of oxygen during the fuel stops. Hence, the greatly improved performance with Mn ore as oxygen carrier is probably explained by the high reactivity of Mn-based carriers with syngas [54], which reduces gasification inhibition.

## 5. Discussion

### 5.1 Experiments with natural gas

The cornerstone of the CLC technology is the development of feasible oxygen carriers which have sufficient mechanical and chemical stability for long periods of time in continuous CLC systems. At the outset of the work in this thesis there was only a limited number of investigations of oxygen carriers in continuous units, and only for limited periods of time. Hence, the experiments conducted with the Ni-based particles in the Gas-10 kW unit is a milestone due to the long-term tests. These demonstrated high mechanical stability of the particles, with lifetimes of up to 33000 h based on loss of fine material after 1000 h of operation. Perhaps equally important, the particles investigated in long-term operation were produced using commercial raw materials and production methods, *i.e.* spray-drying. Hence, the results imply that a well-working oxygen-carrier can be produced at reasonable cost, giving a solid base for an up-scaling and commercialization of the technology.

### 5.2 Experiments with solid fuels

With gaseous fuels complete CO<sub>2</sub> capture is normally obtained in CLC pilot operation, and also very high conversion of fuel to CO<sub>2</sub> and H<sub>2</sub>O has been demonstrated. With solid fuels the situation is different, because of difficulties related to char conversion as well as with fuel feeding. Thus, the slow gasification of char may give incomplete solid fuel conversion due to elutriation of char particles, as well as incomplete CO<sub>2</sub> capture due to loss of char to the air reactor. Moreover solid fuel releases combustible gases inside the fluidized bed, *i.e.* at all locations where fuel or char particles are present. Thus, the contact between combustible gases and oxygen carrier is less efficient, as compared to the case of gaseous fuels where the combustible gases are added from below the fluidized bed. The performance of chemical-looping of solid fuels can be assessed by the following key numbers:

- $\eta_{SF}$ , or the solid fuel conversion, which shows the fraction of carbon added that is converted to gas in the system, thus indicating the loss of unconverted char.
- $\eta_{CC}$ , or the carbon capture, showing the fraction of gaseous carbon leaving the system from the fuel reactor, thus indicating the loss of carbon to the air reactor.
- $\Omega_{OD}$ , or the oxygen demand, which shows the fraction of oxygen missing to achieve complete oxidation of the gases leaving the fuel reactor.

Previous work with solid fuels has clearly indicated moderate performance for these key numbers. Thus, using pet coke in the SF-10 kW,  $\eta_{SF}$  was in the range 55-75%,  $\eta_{CC}$  in the range

68-87% and  $\Omega_{OD}$  in the range 27-36%, [20]. The present work clearly demonstrates the potential for improvements of the performance for CLC of solid fuels:

- $\Omega_{OD}$  is greatly improved with in-bed fuel feed, and a further significant improvement in  $\Omega_{OD}$  is accomplished by using an oxygen carrier with higher reactivity. It is expected that  $\Omega_{OD}$  could be lowered even more by feeding the fuel further down into the bed.
- The use of a more reactive oxygen carrier also had a profound effect on the char gasification rate, resulting in higher  $\eta_{CC}$ . An increase for  $\eta_{CC}$  from around 70% with ilmenite, to as much as 98% with Mn ore was observed for similar residence time. It should be noted that this was also with a fuel, pet coke, well known for low char reactivity, *i.e.* slow char gasification. Moreover, the carbon stripper of the SF-10 kW unit is very primitive, and an effective carbon stripper should be able to improve the carbon capture significantly. Consequently, a good oxygen carrier in combination with an effective carbon stripper should be able to reach very high or even complete carbon capture.
- The increase in char gasification rate also improved  $\eta_{SF}$ . However, the possibilities for reaching high  $\eta_{SF}$  in this unit are small, because of the short riser and the inefficient cyclone releasing large amounts of char particles in the size range 45-90  $\mu\text{m}$ , [19]. In fact, 44% of the added pet coke is smaller than 90  $\mu\text{m}$ , *cf.* Paper VI. A full-scale unit with a riser two orders of magnitude higher, combined with a cyclone efficiently recycling elutriated char, would provide very much longer residence time of the char particles in the system. Thus, it should be possible to achieve a much higher  $\eta_{SF}$ .

It is not expected that it is possible to reach full conversion in the fuel reactor when using solid fuels, unless CLOU materials are used. But a high  $\Omega_{OD}$  is nevertheless important to reduce the treatment needed of exiting gases. To reach full conversion to  $\text{CO}_2$  there are two main options available, (i) adding some oxygen after the fuel reactor or (ii) separation of unconverted gases from  $\text{CO}_2$  in connection with the  $\text{CO}_2$  liquefaction, and recycling of these gases to the fuel reactor as fluidizing gas.

In conclusion, this work clearly demonstrates the potential of reaching high performance in CLC with solid fuels.

## 6. Conclusions

CLC is a prime contender for CO<sub>2</sub> capture because it can achieve CO<sub>2</sub> separation inherently. Alternative capture technologies require cost-intensive separation steps, either down-stream or up-stream of the combustion. The work presented in this thesis involves experimental evaluation of oxygen carriers in continuous reactor systems. The large-scale application of CLC is still dependent upon the availability and performance of oxygen carriers.

### 6.1 Experiments with gaseous fuels

The purpose of the work presented in Papers I-III was to investigate the feasibility of making a good oxygen carrier at a reasonable production cost by using commercially available raw materials and commercial preparation methods. The work focuses primarily on the long-term performance of oxygen carriers in continuous CLC operation. The most important finding is that oxygen-carrier particles prepared from commercially available raw materials by spray-drying were used for > 1000 h of combustion (Paper II) without any observed loss in reactivity or mechanical strength.

#### 6.1.1 Long-term tests in Gas-10 kW using N-IFP (Paper I)

An oxygen carrier produced by spin-flash drying was evaluated during 160 h of fuel operation. High fuel conversion to CO<sub>2</sub> and H<sub>2</sub>O was achieved. The exit gas stream from the fuel reactor contained typically 0.7% CO, 0.3% CH<sub>4</sub> and approximately 1.3% H<sub>2</sub>. Furthermore:

- Investigations of the relationship between CH<sub>4</sub> and circulation confirmed previously presented theories that a large solids flux leads to increased methane concentrations and vice versa.
- No decrease in reactivity was seen during the test period.
- The loss of fines was larger than that observed in previous testing in the CLC unit. The particle lifetime corresponding to the loss of fines was 4500 h.

#### 6.1.2 Long-term tests in Gas-10 kW using N-VITO and N-VITOMg (Paper II)

405 h of fuel operation were accomplished using N-VITO, a particle with NiO (40%<sub>mass</sub>) as active component and NiAl<sub>2</sub>O<sub>4</sub> as inert. Another 611 h of operation were accomplished using a mixture of the used N-VITO particles in combination with a similar particle, N-VITOMg. The reason for mixing the two particles was to optimize the performance with respect to fuel conversion. In general, fuel conversion increased, as expected, with (a) decreased circulation, and (b) increased fuel-reactor temperature. Further conclusions:

- Compared to the operation with only N-VITO, fuel conversion was improved using the oxygen-carrier mixture, although the fraction of CO was higher.
- Using the oxygen-carrier mixture, the methane fraction was typically 0.4-1% and the typical combustion efficiency was 98%.
- No decrease in reactivity was seen during the test period. During an initial period, the reactivity increased.
- The loss of fines decreased slowly throughout the test period. An estimated particle lifetime of 33000 h was calculated from the loss of fines.

### **6.1.3 Comparison of Ni-based oxygen carriers (Paper III)**

A 300-W CLC unit was used to investigate the possibility to optimize the performance of oxygen carriers by using mixed oxygen carrier batches, and results showed that such optimization was possible. The oxygen carriers N-VITO and N-VITOMg were evaluated in batch fluidized-bed experiments, individually and mixed, and the mixture turned out to perform optimally. In order to confirm the results obtained in the batch reactor, N-VITO and a mixture of the two particles were evaluated in the 300-W unit:

- The operation with N-VITO was somewhat unstable, and the fuel conversion was unsatisfactory at  $T_{FR} = 750^{\circ}\text{C}$ , but high at the higher temperatures.
- With the mixture of the two spray-dried particles, operation was stable and, in comparison to the operation with N-VITO, fuel conversion improved at all three temperatures, especially at  $750^{\circ}\text{C}$ . At low circulation, the fraction of unconverted methane was  $< 0.1\%$  both at  $850^{\circ}\text{C}$  and  $950^{\circ}\text{C}$ .
- Furthermore, a third, NiO-based impregnated oxygen carrier was introduced into the mixture in order to improve the methane conversion even further. Excellent conversion of the fuel was obtained at relatively high circulation with this three-particle mixture.

## **6.2 Experiments with solid fuels**

The purpose of the work with solid fuels, Papers IV-VI, was to improve the performance of the existing chemical-looping combustor, increase the level of understanding of CLC with solid fuels by using a variety of different fuels and finally, to investigate to what extent overall performance of the CLC unit could be improved by using a previously untested oxygen carrier with higher reactivity.

### 6.2.1 Batch experiments (Paper IV)

By making batch tests, it was possible to determine (a) oxygen demand associated with syngas from char gasification as well as (b) kinetics of char conversion to gas. Instantaneous rates of char conversion to gas were found to be temperature dependent, as expected. Furthermore:

- The reaction rate constant for char conversion was found to increase with a factor 1.6 - 3.2 between 970°C and 1030°C.
- The minimum oxygen demand, assumed to be the same as the oxygen demand for syngas from char gasification, was found to be 4-5% for pet coke and met coke, and 6-11% for the bituminous fuels.

### 6.2.2. Continuous experiments (Papers V and VI)

The continuous tests were aimed at investigating properties of different oxygen carriers based on natural minerals. The main conclusions are listed below.

- Compared to a base case with only ilmenite, the use of limestone as additive to ilmenite was found to increase the rate of char gasification as well as improving gas conversion. This result was explained by the catalytic effect of limestone on the water-gas shift equilibrium.
- The bituminous coal is more reactive than the pet coke, possibly due to higher porosity. This is manifested as higher gasification efficiency and higher CO<sub>2</sub> capture.
- The new, in-bed fuel feed gave higher gas conversion to CO<sub>2</sub>, mainly due to improved contact between oxygen carrier and volatiles.
- Using bituminous coal, the oxygen demand fell to a minimum of 6% after terminating the fuel feed, indicating high conversion of syngas from char gasification.

#### *Operation with Mn ore*

The new, in-bed fuel feed was used to compare oxygen-carrier properties of ilmenite and manganese ore. With pet coke as fuel, it was found that:

- The use of a manganese ore as oxygen carrier greatly enhanced the rate of gasification, which occurred approximately four times faster than with ilmenite. This is illustrated by the loss of char to the AR, which is reduced from around 28% to 2-6%. In other words, the carbon capture efficiency was as high as 98%.

- Gas conversion also improved significantly using manganese ore. If H<sub>2</sub>S is excluded, the oxygen demand is as low as 10%, which can be compared to the lowest value found for ilmenite, 18%.
- Mechanical stability of the Mn ore was inferior to ilmenite, judged by the production of fines.

## References

---

- [1] United Nations Development Programme, Human Development Report (HDR) 2006
- [2] Statens energimyndighet. Energiläget 2010.
- [3] National Oceanic and Atmospheric Administration (NOAA), Earth System Research Laboratory: Global Monitoring Division. (<http://www.esrl.noaa.gov/>)
- [4] Boden, T.A., G. Marland, and R.J. Andres. 2010. Global, Regional, and National Fossil-Fuel CO<sub>2</sub> Emissions. Carbon Dioxide Information Analysis Center, Oak Ridge National Laboratory, U.S. Department of Energy, Oak Ridge, Tenn., U.S.A..
- [5] IPCC. 2005. IPCC Special Report: Carbon Dioxide Capture and Storage.
- [6] IPCC. 2007. IPCC Fourth Assessment Report (AR4). Working Group I: The Physical Science Basis.
- [7] Anderegg, W., Prall, J., Harold, J., and Schneider, S., Expert credibility in climate change, *Proceedings of the National Academy of Sciences, July 6, 2010 vol. 107 no. 27 12107-12109.*
- [8] Harvey, D. 2000. *Global Warming: The Hard Science*. Pearson Education Limited.
- [9] Lindzen, R., and Choi, Y-S. On the determination of climate feedbacks from ERBE data. *Geophysical Research Letters, VOL. 36, L16705, doi:10.1029/2009GL039628, 2009.*
- [10] Jin, X., Gruber, N., Frenzel, H., Doney, S. C., and McWilliams, J. C., The impact on atmospheric CO<sub>2</sub> of iron fertilization induced changes in the ocean's biological pump, *Biogeosciences, 5, 385–406, 2008.*
- [11] Lewis, W. K., Gilliland, E. R. 1954. Productions of pure carbon dioxide. US Patent No. 2,665,972.
- [12] Ishida, M. and Jin, H. 1994. A new advanced power-generation system using chemical-looping combustion. *Energy* Vol. 19. No. 4. pp. 415-422.
- [13] Lyngfelt, A., Leckner, B., Mattisson, T. 2001. A fluidized-bed combustion process with inherent CO<sub>2</sub> separation - application of chemical-looping combustion. *Chemical Engineering Science* 56:3101-3313.
- [14] Johansson, M., Mattisson, T. and Lyngfelt, A., Comparison of oxygen carriers for chemical-looping combustion. *Thermal Science, 10 (2006) 93-107.*
- [15] Hossain, M., de Lasa, H. Chemical-looping combustion (CLC) for inherent CO<sub>2</sub> separations – a review. *Chemical Engineering Science* 63 (2008) 4433 – 4451.
- [16] Kolbitsch, P., Pröll, T., Hofbauer, H., Modeling of a 120 kW chemical looping combustion reactor system using a Ni-based oxygen carrier. *Chemical Engineering Science, Volume 64, Issue 1, January 2009, Pages 99-108.*
- [17] Abad, A., Adánez, J., García-Labiano, F., de Diego, L. F., Gayán, P. Modeling of the chemical-looping combustion of methane using a Cu-based oxygen-carrier *Combustion and Flame, Volume 157, Issue 3, March 2010, Pages 602-615.*
- [18] Berguerand N, Lyngfelt A. Design and operation of a 10 kW<sub>th</sub> chemical-looping combustor for solid fuels – Testing with South African coal. *Fuel* 2008; 87:2713-2726.
- [19] Berguerand N, Lyngfelt A. The use of Petroleum coke in a 10 kW<sub>th</sub> Chemical-Looping Combustor. *International Journal of Greenhouse Gas Control* 2008; 2(2):169-179.
- [20] Berguerand N, Lyngfelt A. Chemical-Looping Combustion of Petroleum Coke using Ilmenite in a 10 kW<sub>th</sub> unit – High Temperature Operation. *Energy&Fuels* 2009; 23(10): 5257-5268.
- [21] Berguerand, N, and Lyngfelt, A., Operation in a 10 kW<sub>th</sub> Chemical-Looping Combustor for Solid Fuel – Testing with a Mexican Petroleum Coke, *Energy Procedia* 1 (2009) 407-414.
- [22] Shen L, Wu J, Xiao J. Experiments on Chemical-looping Combustion of Coal with a NiO based Oxygen Carrier. *Combustion and Flame* 2009; 156(3): 721-728.
- [23] Shen, L, Wu, J., Xiao, J., Song, Q., and Xiao, R., (2009) Chemical looping combustion of biomass in a 10 kW<sub>th</sub> reactor with iron oxide as an oxygen carrier, *Energy Fuels* 23 2498-2505.
- [24] Shen, L., Wu, J., Gao, Z., and Xiao, J., (2009) Reactivity deterioration of NiO/Al<sub>2</sub>O<sub>3</sub> oxygen carrier for chemical looping combustion of coal in a 10 kW<sub>th</sub> reactor, *Combustion and Flame* 156, 1377-1385.

- 
- [25] Wu, J., Shen, L., Xiao, J., Wang, L., and Hao, J., (2009) Chemical looping combustion of sawdust in a 10 kW<sub>th</sub> interconnected fluidized bed, *Huagong Xuebao/CIESC Journal* 60:8, 2080-2088.
- [26] Cuadrat, A., Abad, A., García-Labiano, F., Gayán, P., de Diego, L-F, Adánez, J. Effect of operating conditions in Chemical-Looping Combustion of Coal in a 500 W<sub>th</sub> unit. *Submitted for publication*.
- [27] Fang H., Haibin L., Zengli Z. (2009) Advancements in development of chemical looping combustion (CLC): A review, *International Journal of Chemical Engineering, Volume 2009, Article ID 710515, 16 pages*.
- [28] Lyngfelt, A., Oxygen carriers for chemical-looping combustion - 4000 h of operational experience, Accepted for publication in *Oil & Gas Science and Technology - Revue d'IFP Energies nouvelles*.
- [29] Lyngfelt, A., and Mattisson, T., Materials for chemical-looping combustion, Accepted for publication in *CCS POWER PLANTS (Stolten)*.
- [30] Leckner, B. Fluidized bed combustion: Mixing and pollutant limitation *Progress in Energy and Combustion Science, Volume 24, Issue 1, 1998, Pages 31-61*
- [31] Buecker, B., 2002. *Basics of boiler and HRSG design*. PennWell Corporation. Tulsa, Oklahoma.
- [32] Hotta, A. Foster Wheeler's Solutions for Large Scale CFB Boiler Technology: Features and Operational Performance of Łagisza 460 MW<sub>e</sub> CFB Boiler. Proceedings of the 20<sup>th</sup> International Conference on Fluidized Bed Combustion 2010, Part 1, 59-70
- [33] Reh. L. Development potentials and research needs in circulating fluidized bed combustion, *China Particuology Vol. 1, No. 5, 185-200, 2003*.
- [34] Wolf, J. 2004. CO<sub>2</sub> mitigation in advanced power cycles, PhD Thesis, Department of Chemical Engineering and Technology. Royal Institute of Technology, Stockholm, Sweden.
- [35] Naqvi, R. 2006. Analysis of Natural Gas-fired Power Cycles with Chemical Looping Combustion for CO<sub>2</sub> Capture, PhD Thesis, Department of Energy and Process Engineering, Norwegian University of Science and Technology, Trondheim, Norway.
- [36] Kolbitsch, P., Pröll, T., Bolhar-Nordenkamp, J., Hofbauer, H. 2008. Operating experience with chemical looping combustion in a 120kW dual circulating fluidized bed (DCFB) unit. GHGT-9: 9<sup>th</sup> International Conference on Greenhouse Gas Control Technologies, 16-20 November 2008.
- [37] Arnold, C., (representing the Standard Oil Development Company), *Process for the Production of Carbon Monoxide and Hydrogen*, UK patent 636.206 published April 26, 1950.
- [38] Mattisson, T., Lyngfelt, A. 2001. Applications of chemical-looping combustion with capture of CO<sub>2</sub>. Proceedings of the 2<sup>nd</sup> Nordic Minisymposium on Carbon Dioxide Capture and Storage, Göteborg, Sweden.
- [39] Mattisson, T., Zafar, Q., Lyngfelt, A., and Gevert, B. 2004. Integrated hydrogen and power production from natural gas with CO<sub>2</sub> capture. 15th World Hydrogen Energy Conference, Yokohama, 27th June-2nd July, 2004.
- [40] Zafar, Q. 2005. *Investigation of oxygen carrier materials for Chemical-Looping Reforming*, Licentiate Thesis, Department of Chemical and Biological Engineering, Chalmers University of Technology, Göteborg.
- [41] Johansson, R. 2003. *Integrerad vätgas- och kraftproduktion utan utsläpp av koldioxid – tillämpning av chemical-looping combustion*, Master Thesis, Chalmers University of Technology, Göteborg, Sweden.
- [42] Rydén, M. 2008. *Hydrogen production from fossil fuels with carbon dioxide capture, using chemical-looping technologies*, PhD Thesis, Department of Energy and Environment, Division of Energy Conversion, Chalmers University of Technology, Göteborg, Sweden.
- [43] de Diego, L. F., Ortiz, M., Adánez, J., García-Labiano, F., Abad, A., Gayán, P. 2008. Synthesis gas generation by chemical-looping reforming in a batch fluidized bed reactor using Ni-based oxygen carriers. *Chemical Engineering Journal* Volume 144, Issue 2, Pages 289-298.
- [44] Wen, C. Y., Lee, E. S., Ed., *Coal Conversion Technology*, Addison-Wesley, Publishing Co., Reading, MA, 1979.

- 
- [45] Jerndal, E., Leion, H., Axelsson, L., Ekvall, T., Hedberg, M., Johansson, K., Källén, M., Svensson, R., Mattisson, T., and Lyngfelt, A., Using Low-Cost Iron-Based Materials as Oxygen Carriers for Chemical-Looping Combustion, Accepted for publication in *Oil & Gas Science and Technology - Rev. IFP*.
- [46] Leion, H., Lyngfelt, A., Johansson, M., Jerndal, E., Mattisson, T. 2008. The use of ilmenite as an oxygen carrier in chemical-looping combustion. *Chemical Engineering Research and Design* 86: 1017-1026.
- [47] Johansson, M., Mattisson, T., Rydén, M. and Lyngfelt, A. 2006. Carbon Capture via Chemical-Looping Combustion and Reforming. *International Seminar on Carbon Sequestration and Climate Change*, Rio de Janeiro, Brazil, 24-27 October 2006.
- [48] Jerndal, E., Mattisson, T., and Lyngfelt, A. 2006. Thermal Analysis of Chemical-Looping Combustion. *Chemical Engineering Research and Design* 84:795-806.
- [49] Cho, P., Mattisson, T. and Lyngfelt, A. 2004. Comparison of iron-, nickel-, copper- and manganese-based oxygen carriers for chemical-looping combustion. *Fuel* 83:1215-1225.
- [50] Ishida, M., Yamamoto, M., Ohba, T. 2002. Experimental results of chemical-looping combustion with NiO/NiAl<sub>2</sub>O<sub>4</sub> particle circulation at 1200 °C. *Energy Conversion and Management* 43:1469-1478.
- [51] de Diego, L. F., García-Labiano, F., Adánez, A., Gayán, P., Abad, A., Corbella, B. M., Palacios, J. M. 2004. Development of Cu-based oxygen carriers for chemical-looping combustion. *Fuel* 83:1749-1757.
- [52] Villa, R., Cristiani, C., Groppi, G., Lietti, L., Forzatti, P., Cornaro, U., Rossini, S. Ni based mixed oxide materials for CH<sub>4</sub> oxidation under redox cycle conditions. *Journal of Molecular Catalysis A: Chemical*. Volumes 204-205, 2006, Pages 637-646.
- [53] Pröll, T., Mayer, K., Bolhàr-Nordenkampf, J., Kolbitsch, P., Mattisson, T. and Lyngfelt, A., Hofbauer, H., Natural minerals as oxygen carriers for chemical looping combustion in a dual circulating fluidized bed system, *Energy Procedia 1 (2009) 27-34*.
- [54] Leion, H., Mattisson, T. and Lyngfelt, A., The use of ores and industrial products as oxygen carriers in chemical-looping combustion, *Energy & Fuels 23 (2009) 2307-2315*.
- [55] Rydén, M., Lyngfelt, A., and Mattisson, T., Combined manganese/iron oxides as oxygen carrier for chemical looping combustion with oxygen uncoupling (CLOU) in a circulating fluidized bed reactor system, *Energy Procedia, Volume 4, 2011, Pages 341-348*.
- [56] Mattisson, T., Johansson, M., and Lyngfelt, A. The use of NiO as an oxygen carrier in chemical-looping combustion. *Fuel* 85 (2006):736-747.
- [57] Lyngfelt, A., Mattisson, T. Trestegsforbränning för avskiljning av koldioxid; 2005.
- [58] Lewis, W., Gilliland, E., and Sweeney, M., Gasification of carbon – Metal oxides in a fluidized powder bed, *Chem. Eng. Progress* 47:5 (1951) 251-256.
- [59] Mattisson, T., Lyngfelt, A., and Leion, H., Chemical-Looping with Oxygen Uncoupling for Combustion of Solid Fuels, *International Journal of Greenhouse Gas Control* 3 (2009) 11-19.
- [60] Shulman, A., Cleverstam, E., Mattisson, T., and Lyngfelt, A., Chemical – Looping with Oxygen Uncoupling using Mn/Mg-based Oxygen Carriers for Methane Combustion, *Fuel* 90 (2011) 941-950.
- [61] Shulman, A., Cleverstam, E., Mattisson, T., and Lyngfelt, A., Manganese/Iron, Manganese /Nickel and Manganese /Silicon Oxides Used in Chemical – Looping With Oxygen Uncoupling (CLOU) for Combustion of Methane, *Energy & Fuels* 23 (2009) 5269-5275.
- [62] Azimi, G., Leion, H., Mattisson, T. and Lyngfelt, A., Chemical-Looping with Oxygen Uncoupling using combined Mn-Fe oxides, testing in batch fluidized bed, *Energy Procedia, Volume 4, 2011, Pages 370-377*.
- [63] Lambert, A., Delquié, C., Clémeneçon, I., Comte, E., Lefebvre, V., Rousseau, J., Durand, B. Synthesis and characterization of bimetallic Fe/Mn oxides for chemical looping combustion . *Energy Procedia, Volume 1, Issue 1, February 2009, Pages 375-381*.

- 
- [64] Leion, H., Larring, Y., Bakken, E., Mattisson, T., Bredesen, R., and Lyngfelt, A., The use of  $\text{CaMn}_{0.875}\text{Ti}_{0.125}\text{O}_3$  as oxygen carrier in Chemical-Looping with Oxygen Uncoupling (CLOU), *Energy & Fuels* **23** (2009) 5276-5283.
- [65] Rydén, M., Lyngfelt, A., and Mattisson, T.,  $\text{CaMn}_{0.875}\text{Ti}_{0.125}\text{O}_3$  as oxygen carrier for chemical-looping combustion with oxygen uncoupling (CLOU) – experiments in continuously operating fluidized bed reactor system, *Int. Journal of Greenhouse Gas Control* **5** (2011) 356-366.
- [66] Johansson, M., Mattisson, T. and Lyngfelt, A., Investigation of  $\text{Mn}_3\text{O}_4$  with stabilized  $\text{ZrO}_2$  for chemical-looping combustion. *Chemical Engineering Research and Design* **84** (2006) 807-818.
- [67] Cuadrat, A., Abad, A., Adánez, J., de Diego, L., García-Labiano, F., Gayán, P., Behaviour of Ilmenite as Oxygen Carrier in Chemical-Looping Combustion. Clean Coal Technology Conference, 2009.
- [68] Johansson, E., Lyngfelt, A., Mattisson, T. and Johnsson, F. 2002. A circulating fluidized bed combustor system with inherent  $\text{CO}_2$  separation - application of chemical looping combustion. 7<sup>th</sup> *Int. Conf. on Circulating Fluidized Beds*, Niagara Falls, Ontario, May 5-7, 2002, 717-724.
- [69] Markström, P., Berguerand, N., and Lyngfelt, A., The Application of a Multistage-Bed Model for Residence-Time Analysis in Chemical-Looping Combustion of Solid Fuel, *Chemical Engineering Science, Volume 65, Issue 18, 15 September 2010, Pages 5055-5066*.
- [70] Kunii, D., Levenspiel, O. 1991. *Fluidization Engineering*. Reed Publishing Inc., Stoneham.
- [71] Lyngfelt, A., Kronberger, B., Adanez, J., Morin, J.-X., and Hurst, P. 2005. The GRACE project. Development of oxygen carrier particles for chemical-looping combustion. Design and operation of a 10 kW chemical-looping combustor. *Greenhouse Gas Control Technologies 7:115-123* (7<sup>th</sup> International Conference on Greenhouse Gas Control Technologies, Vancouver, Canada, 5<sup>th</sup>-9<sup>th</sup> September 2004).
- [72] Johansson, M., Mattisson, T. and Lyngfelt, A. 2006. The use of  $\text{NiO/NiAl}_2\text{O}_4$  particles in a 10 kW chemical-looping combustor. *Ind. Eng. Chem. Res.* **45**:5911-5919.
- [73] Lyngfelt, A., and Thunman, H., 2005. Construction and 100 h of operational experience of a 10 kW chemical looping combustor. In: Thomas, D. (Ed.), *Carbon Dioxide Capture for Storage in Deep Geologic Formations—Results from the  $\text{CO}_2$  Capture Project. Capture and Separation of Carbon Dioxide From Combustion Sources, vol. 1* Elsevier Science, London, pp. 625–646 (Chapter 36).
- [74] Leion, H., 2008, Capture of  $\text{CO}_2$  from Solid Fuels using Chemical-Looping Combustion and Chemical-Looping with Oxygen Uncoupling, *PhD Thesis, Dept. of Chemical and Biological Engineering, Environmental Inorganic Chemistry, Chalmers University of Technology, Göteborg, Sweden*.
- [75] Jerndal, E., Mattisson, T., Thijs, I., Snijkers, F., Lyngfelt, A. 2008. NiO particles with Ca and Mg based additives produced by spray-drying as oxygen carriers for chemical-looping combustion. 9<sup>th</sup> International Conference on Greenhouse Gas Control Technologies, 16 - 20 November 2008.
- [76] Sehested, J. 2003. Sintering of nickel steam-reforming catalysts. *Journal of catalysis* **271**:417-426.
- [77] Dueso, C., de Diego, L. F., García-Labiano, F., Gayán, P., Abad, A., Adánez, J. 2008. Methane Combustion in a 500 W<sub>th</sub> Chemical-Looping Combustion System Using an Impregnated Ni-based Oxygen Carrier. Submitted for publication.

